AD NUMBER

AD802567

LIMITATION CHANGES

TO:

Approved for public release; distribution is unlimited.

FROM:

Distribution authorized to U.S. Gov't. agencies and their contractors; Critical Technology; SEP 1966. Other requests shall be referred to Air Force Rocket Propulsion Laboratory, ATTN: RPPR-STINFO, Edwards AFB, CA 93523. This document contains export-controlled technical data.

AUTHORITY

AFRPL ltr dtd 20 Dec 1971

Report No AFRPL-TR-66-220

INVESTIGATION OF THE THERMODYNAMIC PROPERTIES OF ROCKET EXHAUST PRODUCTS

Milton Farber, M A Greenbaum, Margaret A Frisch, et al

FINAL REPORT
Contract AF 04(611)-10929
September 1966

Department of the Air Force
Air Force Rocket Propulsion Laboratory (AFSC)
Edwards, California 93523

Rocket Power, Inc
2275 E Foothill Blvd
Pasadena, California 91107

Report No. AFRPL-TR-66-220

INVESTIGATION OF THE THERMODYNAMIC PROPERTIES OF ROCKET EXHAUST PRODUCTS

FINAL REPORT

Contract AF 04(611)-10929

September 1966

Department of the Air Force
Air Force Rocket Propulsion Laboratory (AFSC)
Edwards, California 93523

Authors:
Milton Farber
M. A. Greenbaum
M. A. Frisch
H. C. Ko
L. B. Marantz
B. Chai
G. Grenier
R. Yates

Rocket Power, Inc.
2275 E. Foothill Blvd.
Pasadena, California 91107

FOREWORD

This report presents details of the work performed under Contract AF 04(611)-10929 during the period August 1, 1965 through July 31, 1966 at the Rocket Power, Inc. Research Laboratories, 2275 E. Foothill Blvd., Pasadena, California 91107. The technical monitor of this program was Mr. Curtis C. Selph, RPCL, Air Force Rocket Propulsion Laboratory, Air Force Systems Command, Edwards, California.

This technical report has been reviewed and is approved.

W. H. Ebelke, Colonel, USAF
Chief, Propellant Division

ABSTRACT

A thermodynamic research program for the past twelve months has resulted in thermal data for the high temperature stable species BeOH(g), HBO(g), B_2O_3(g), HOBO(g), $AlCl_2$(g) and Al_2Cl_4(g). In addition, infrared spectral data have been obtained for $Be(OH)_2$(g).

SUMMARY OF THERMODYNAMIC DATA

BeOH(g)

	2nd Law	3rd Law
$\Delta H^\circ_{f2235^\circ K}$	-55.7 ± 3.8 kcal/mole	$-56.7 \pm .5$ kcal/mole
$\Delta H^\circ_{f298^\circ K}$	-46.8 ± 3.8 kcal/mole	$-48.2 \pm .5$ kcal/mole
$S^\circ_{2235^\circ K}$	75.3 ± 1.7 cal/deg/mole	
$S^\circ_{298^\circ K}$	54.0 ± 1.7 cal/deg/mole	53.3 cal/deg/mole (JANAF)

$AlCl_2$(g)

$\Delta H^\circ_{f298^\circ K}$	-66.0 ± 3 kcal/mole

Al_2Cl_4(g)

$\Delta H^\circ_{f900^\circ K}$	-194.8 ± 1.0 kcal/mole
$\Delta H^\circ_{f298^\circ K}$	-194.0 ± 5 kcal/mole
$S^\circ_{900^\circ K}$	116 ± 1.0 cal/deg/mole
$S^\circ_{298^\circ K}$	90 ± 5 cal/deg/mole

HBO(g)

	2nd Law	3rd Law
$\Delta H^{\circ}_{f1260^{\circ}K}$	-51 ± 3 kcal/mole	
$\Delta H^{\circ}_{f298^{\circ}K}$	-50 ± 3 kcal/mole	

$B_2O_3(g)$

$\Delta H_{v1320^{\circ}K}$	86.3 ± 2 kcal/mole
$\Delta H_{v298^{\circ}K}$	93.6 ± 2 kcal/mole

HOBO(g)

$\Delta H^{\circ}_{f1320^{\circ}K}$	-135.9 ± 2 kcal/mole
$\Delta H^{\circ}_{f298^{\circ}K}$	-133.5 ± 2 kcal/mole

$Be(OH)_2(g)$

Experimental infrared active vibrational frequency: 649 cm^{-1}

Estimated vibrational frequencies, bent model:

3600	1100	600
3500	900	600
1600	700	300

$S^{\circ}_{1705^{\circ}K}$	93.3 cal/deg/mole (bent model)
$S^{\circ}_{298^{\circ}K}$	60.6 cal/deg/mole (bent model)

TABLE OF CONTENTS

FIGURES

I. INTRODUCTION

The extensive research and development efforts in the area of high energy propellant systems, solid, liquid and hybrid, have led to consideration of an increasingly large number of compounds containing an ever-widening spectrum of the elements. The accurate theoretical evaluation of these new propellant systems in terms of specific impulse, range and similar parameters, requires a knowledge of the thermodynamic properties of the reactants (heat of formation, ΔH_f, is the prime requisite here) and the thermodynamic and physical properties of all the possible products. Among the values needed are heat of formation, entropy, heat capacity, melting point, boiling point, and heats of vaporization, fusion and sublimation. Since the temperatures generally encountered in rockets and missiles fall in the range of 2000-5000°K the necessary thermodynamic properties for the exhaust products must be known in this temperature range.

The existence of thermodynamic data, whether theoretical or experimental, in the range of 20-600°K for a given compound is not sufficient to permit the accurate theoretical evaluation of a propellant system which, on combustion, might form this compound at temperatures of 3000°K. Extrapolation of thermodynamic data over these temperature spans, i.e., 600 to 3000°K, are usually inaccurate. Of even greater importance is the fact that a large number of species produced in the combustion of propellants do not even exist at lower temperatures and thus their properties can only be determined at the high temperatures where they exist. It is for these reasons that research programs have been undertaken to determine the physical and thermodynamic properties of those species expected to be formed by the combustion of propellants.

The current interest in the use of the light metals and their compounds (Li, Be, Mg, Al, B and their hydrides) as fuels or additives in solid or hybrid propellants, has prompted the inauguration of numerous research programs designed to determine the requisite thermodynamic and physical properties of compounds arising from interaction of the metals with the oxidizers employed (generally oxygen or fluorine compounds). Thus, species of prime interest are those arising from reaction of a metal ion with fluorine, oxygen, nitrogen or combinations of these atoms. During the past 12 months thermal data was obtained for the high temperature stable species, BeOH(g), HBO(g), $AlCl_2(g)$ and $Al_2Cl_4(g)$. In addition, infrared spectral data were obtained for $Be(OH)_2(g)$. All thermodynamic values reported at 298°K as well as those at the specified temperatures were calculated using the latest JANAF Tables[1], i.e. those available as of July 31, 1966 except where indicated in the text.

II. THERMODYNAMIC PROPERTIES OF BeOH(g)

A. Introduction

The literature does not report a value for the heat of formation for the subhydroxide, BeOH(g). However, the current JANAF Tables[1] report a value of -25 ± 10 kcal/mole for ΔH_{f298} of BeOH(g). This value is based on a minimum value obtained from a mass spectrometric study[2] of the reaction

$$Be_2O(g) + H_2O(g) = 2BeOH(g) \qquad (1)$$

Prior estimates based on bond energy relationships were reported in preceding JANAF gray Tables[3] as -41 ± 15 kcal/mole for ΔH_{f298} of BeOH(g). Because of these rather large uncertainties and the fact that no values for the thermodynamic properties of BeOH can be found in the literature, a study of the reaction between solid beryllium oxide and gaseous hydrogen was undertaken in this laboratory. The reaction was studied employing the molecular flow effusion method[4] in the temperature range 2107°K to 2368°K.

B. Experimental

1. Apparatus

A high temperature carbon rod furnace was assembled in a high vacuum system. The rods were supported vertically by tantalum sheets (five layers at the top and six layers at the bottom). Alumina caps were used to insulate the rods from the tantalum sheets. The carbon rods were shielded by five cylindrical layers of 5 mil tantalum separated by 1/4" graphite spacers. The inner and outer shields were 2-1/2" and 4-1/2" in diameter, respectively. Tantalum bolts and graphite spacers supported every shield. The entire assembly was supported from the brass plate base by three 1/4" diameter stainless steel rods attached to the outer shield. The leads for the carbon rod heating unit were extended through the five shields and attached to two copper rods, which were connected to the insulated feedthroughs attached to the brass plate. A detailed diagram of the apparatus is presented in Fig. 1.

The reaction cell was a 2" long BeO tube closed at one end, with an o.d. of approximately 0.4", and an i.d. of approximately 0.3". A hole approximately 1 mm in diameter was drilled through the closed end of the tube. The exact dimensions of the cell hole diameter and thickness were measured with a traveling microscope. Two BeO cells with different hole dimensions (as given in Table I) were employed for the series of experiments.

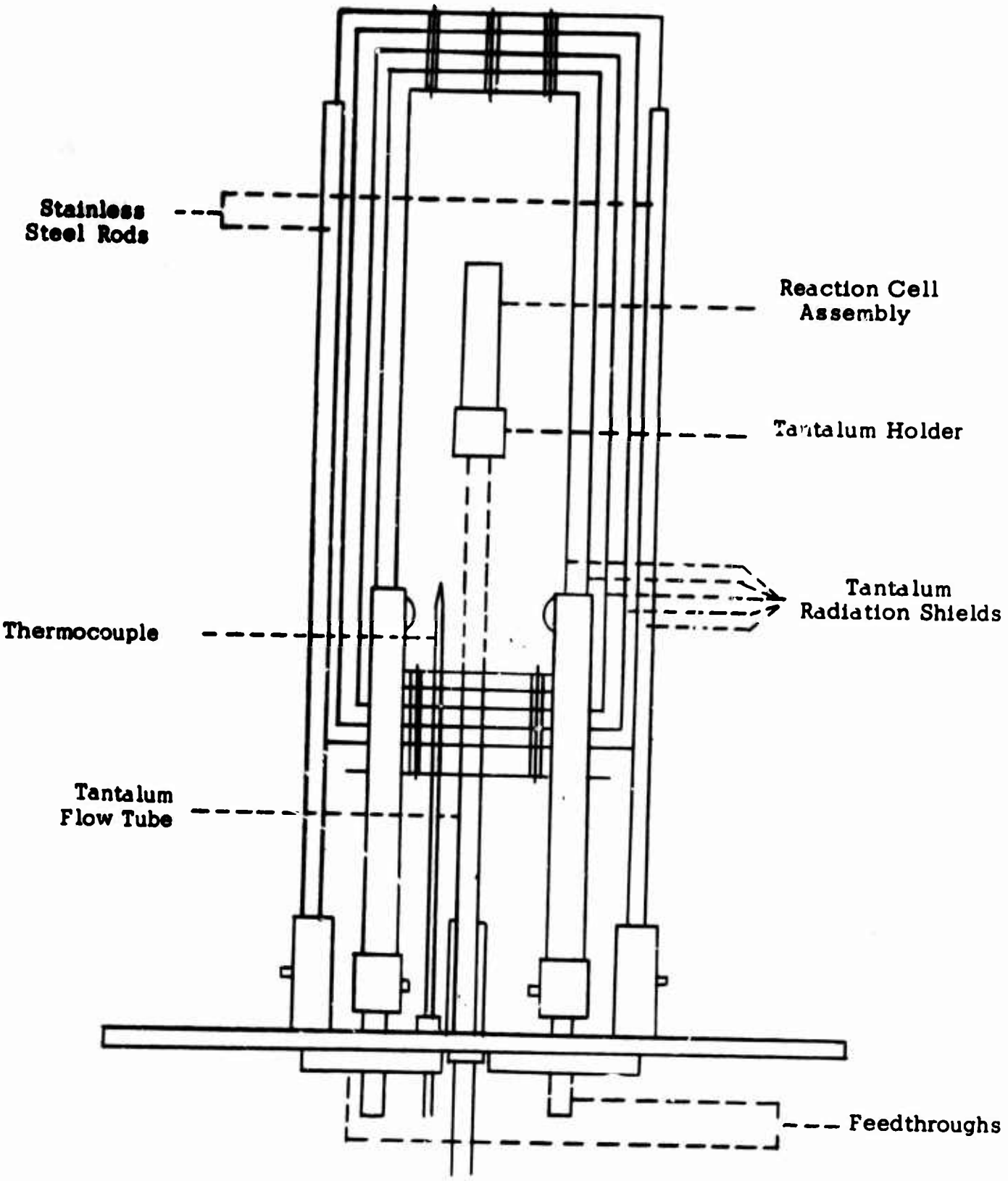

Fig. 1 Schematic Diagram of Furnace Assembly
(side view) for BeOH Studies

The cell was loosely covered with a rhenium cell which had a 1.5 diameter mm hole drilled through the closed end. This rhenium cell in turn was covered with a tantalum cell with a 1.5 mm orifice at the center of the closed end. The entire unit was inserted tightly into a tantalum holder which was fitted to the end of the 1/4" o.d. tantalum flow tube (c.f. Fig. 1). A rhenium foil insert with a 0.2 mm hole was placed over the tantalum tube inlet to prevent flow of species to the tantalum tube. The flow tube penetrated the bottom tantalum sheets of the furnace and a thermocouple fabricated from tungsten, 5% rhenium-tungsten, 26% rhenium wire was used as the temperature sensing element. This thermocouple was inserted approximately 1" inside the inner shield at the bottom of the furnace. The temperature of the cell was measured with an optical pyrometer through a window at the top of the furnace. This measurement was checked against a calibrated thermocouple which was placed inside the cell just below the effusion hole. This thermocouple was checked against a calibrated Pt-Pt, 10% Rh. thermocouple. The results showed that at the experimental temperature range the deviation was within 5 degrees of the standard NBS values. Experiments were performed at 30° intervals for the total of more than 30 performed over the 300° temperature range. The 30° differential temperatures were reproducible to $\pm$ 2 degrees.

The entire furnace assembly was fitted into a 17" long stainless steel cross pipe with 10-1/2" dia. brass plates at the vertical ends and 4" dia. flanges at the side arms. One of the side arms was connected to the pumping system, the other to the ionization and thermocouple gauges. The temperature of the cell could also be measured with an optical pyrometer by viewing through a quartz plate fitted at the top end plate of the pipe. The pressure of the system was usually maintained in the region of 10^{-6} to 10^{-7} mm Hg.

An 8 liter tank was filled with hydrogen (99.999% ultra pure grade) at the commencement of each H_2 experiment. A calibrated gauge was connected to the tank to permit calculation of the amount of hydrogen used during the run. A metering valve was connected to the line immediately prior to the hydrogen entering the flow tube. Approximately the same valve reading was used for each run to insure that the amount of hydrogen used would be fairly constant.

A schematic diagram of the entire apparatus is presented in Fig. 2

2. Procedure

In the temperature range of these experiments BeO has an appreciable weight loss due to vaporization, therefore, a blank run in which no

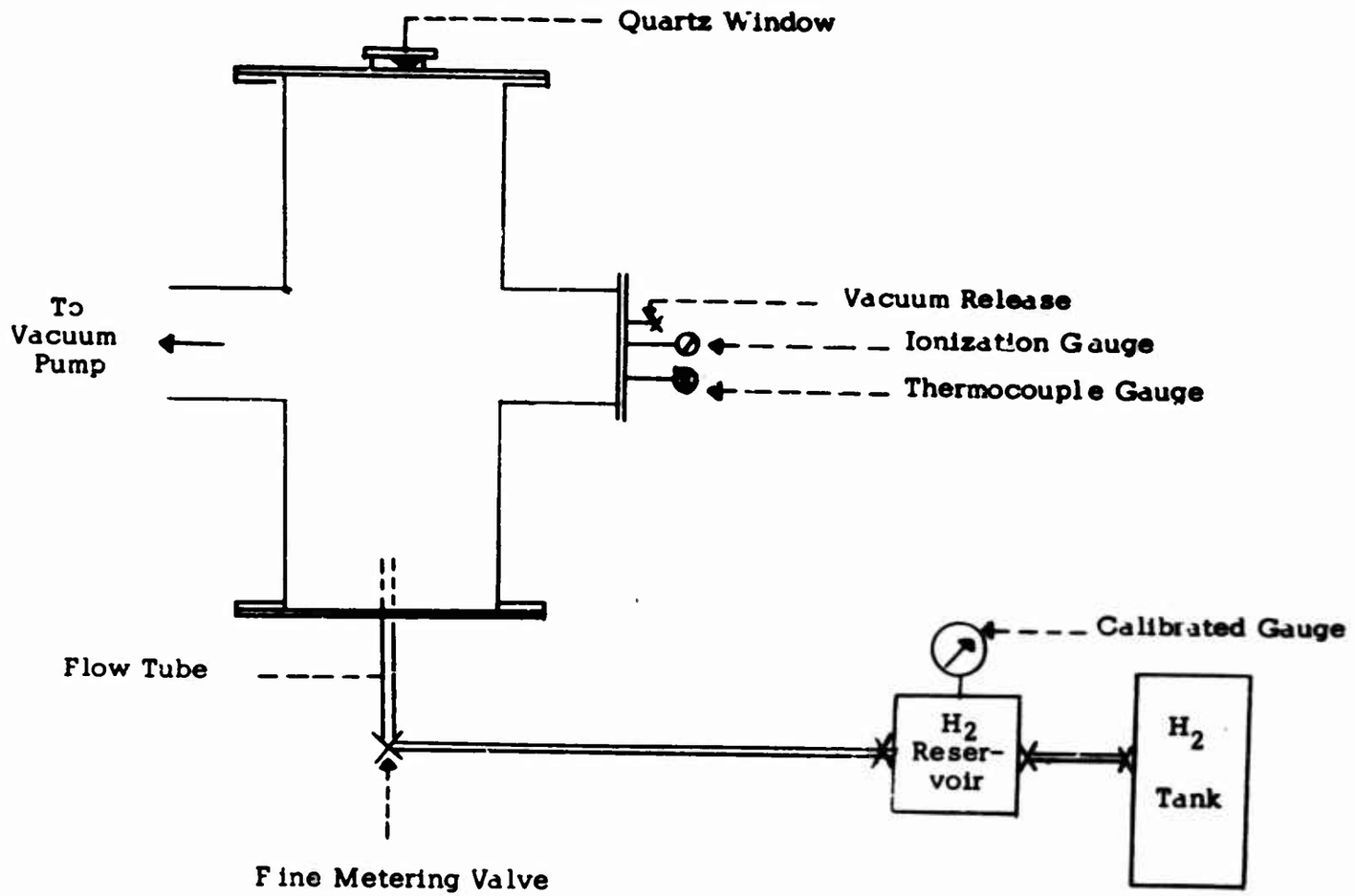

Fig. 2 Schematic Diagram of the Entire Apparatus for BeOH Studies

hydrogen was passed through was performed at each temperature to determine the weight loss of BeO due to vaporization alone. The BeO cell was weighed and the reaction assembly was placed in the system. The system was pumped down to the desired pressure, heating was commenced and a constant temperature was maintained at a desired value. The blank or hydrogen experiment was then begun. Upon completion of the experiment, the system was allowed to cool down to near room temperature and the cell was removed and reweighed. Initial and final readings of the pressure in the hydrogen tank of calibrated volume were recorded. In this manner the number of moles of $H_2(g)$ used in each run was calculated.

C. Discussion

After a considerable number of preliminary experiments were performed to establish that a reaction was indeed occurring between H_2 and BeO, a series of over 30 experiments was made with two effusion cells over a 300° temperature range. Experiments below $2100^{\circ}K$ yielded weight losses too small from which to obtain accurate data. Consequently, the experimental temperature range was chosen as 2107 to $2368^{\circ}K$. The experiments were performed at 30° temperature intervals and in random fashion. Blank runs were made before and after each H_2-BeO reaction experiment. The data for these experiments are presented in Table II.

Although the two cells had different orifice dimensions, a further check for the establishment of equilibrium was made using BeO chips inside the BeO cell. The weight loss results for these experiments were essentially the same as those for the empty cells. Thus, within the experimental error, the surface area of several sq. cm. of the cells was large enough (i.e., reaction area to orifice area greater than 1000, to establish equilibrium with the hydrogen.

Having established that H_2 is reacting with the BeO, the treatment of the data requires a knowledge of the several equilibria that may be involved.

The primary reaction for the formation of BeOH employing H_2 is

$$BeO(c) + 1/2H_2(g) = BeOH(g) \qquad (2)$$

Also to be considered are the reactions

$$BeO(c) + H_2(g) = Be(g) + H_2O(g) \qquad (3)$$

and

$$2BeO(c) + H_2(g) = Be_2O(g) + H_2O \qquad (4)$$

and the dissociation of hydrogen

$$1/2H_2(g) = H(g) \qquad (5)$$

Of secondary importance is the reaction to form the hydroxide from the water formed as a result of reaction (3)

$$BeO(c) + H_2O(g) = Be(OH)_2(g) \qquad (6)$$

The measured quantities for an experiment included the weight loss of BeO and the number of moles of elemental hydrogen employed in the reaction. The total number of moles of H_2, $n_{T(H_2)}$ entering the reaction zone is distributed over the reactions (2), (3) and (5) as

$$n_{T(H_2)} = {}^{1/2}n_{BeOH} + {}^{n}H_2O + {}^{2n}H + {}^{n}H_2 \qquad (7)$$

After consideration for the weight loss of BeO due to vaporization, the remainder of the weight loss of BeO could be attributed to reactions (2), (3), (4) and (6). The weight loss that would be attributed to reaction (6) as a result of the water formed in reaction (3) was negligible in the temperature range studied.[5] Calculations also showed that the contribution due to reaction (4) was negligible. The value reported for the vaporization of liquid beryllium (ΔH_v of Be = 75.38 at 298°K kcal/mole) in the JANAF Tables is based on several recent measurements.[6-10] Employing this value calculations were made for the weight loss of BeO resulting from reaction (3). The remaining weight loss of BeO was attributed to the formation of BeOH. In all experiments the total pressure inside the cell ranged from approximately 0.4 to 0.8 mm. Mean free path calculations in the experimental temperature range indicate that for the cell dimensions the flow for this pressure range is molecular. Therefore, all calculations were based on the modified Knudsen equation

$$P = \frac{17.14G}{W_o At}\sqrt{\frac{T}{M}} \qquad (8)$$

where P is pressure in mm of Hg for the species inside the cell.

G is the weight, in grams, of the gas species escaping through the effusion hole

W_o is the Clausing factor. The dimensions of the cell orifice are given in Table I from which the Clausing factor was calculated as given in Dushman.[11]

A is the area, in cm^2, of the effusion hole

t is the total time of reaction, in seconds

T is temperature in ^oK

M is the molecular weight of the species

The contribution to the weight loss due to reaction (3) was approximately 10 %. Although the vaporization data for Be is quite definitive, it was decided to perform a further check to ascertain that the major reaction was not reaction (3). This check is based on the pronounced effect on reaction (3) which can be brought about by adding a small amount of water vapor to the H_2. A calculation showed that at 2235°K and a total pressure of 0.7 mm of Hg the addition of 3 mole percent water would cause a 75% reduction in weight loss, if this weight loss were due primarily to reaction (3). Such a reduction would occur despite the simultaneous enhancement of reaction (6). This water percentage represents an optimum since at higher percentages the ascendancy of reaction (6) begins to outweigh the reduction in reaction (3).

Thus for a 110 min. run at 2235°K and 0.7 mm total pressure, calculations based on JANAF data[1] for the formation of Be and water as a result of the reaction of hydrogen and BeO would predict a weight loss of 0.74 mg of BeO, while the 3 mole percent water and 97 mole percent H_2 mixture experiment would predict a weight loss of 0.2 mg of BeO. Since the total weight loss in the pure hydrogen experiments at this temperature ranged between 8 and 9 mg, a reduction of 6 to 7 mg would be expected if Be were the chief product formed. However, if the JANAF data for the Be correction were fairly accurate, a negligible change would be expected in the water experiments. Two water experiments (3 mole percent) were performed. The weight losses were 9.6 and 10.1 mg respectively, while the pure hydrogen experiments recorded weight losses of 8.1 and 8.8 mg, respectively.

Although a decrease of 0.5 mg was theoretically predicted, an actual increase of from 0.8 to 2 mg occurred. An examination of the 30 experiments performed in a 300° temperature range, shows that this discrepancy between the actual change and the predicted change of weight losses due to the addition of H_2O is within the scatter of the pure hydrogen experiments, i.e. 1 to 2 mg reproducibility at a given temperature.

The results of the water experiments indicated that use of the published value for the heat of vaporization of Be would be valid. Therefore, a weight loss of BeO was calculated for reaction (3) by means of the Knudsen equation (8) and the JANAF tables for the thermal data. The remaining weight loss of BeO was assumed to be due to the formation of BeOH. The partial pressure of H_2 shown in column 7 of Table III was calculated from the value of n_{H_2} obtained from equation (7). The partial pressure of BeOH(g) was then calculated and an equilibrium constant was obtained for reaction (2). These calculations are presented in Table III.

A plot of the experimental data in Table III in the form of log K_2 vs 1/T is presented in Fig. 3. A least squares analysis of the data yields a value for the slope of the line which corresponds to 88.3 $\pm$ 3.8 kcal for ΔH_r at the average temperature of 2235°K. Similarly, a value for $\Delta S_{r2235^\circ K}$ of 27.4 $\pm$ 1.7 cal/deg is obtained from the intercept of the curve. Employing the available thermodynamic values and thermal functions for BeO(c), H_2(g) and thermal functions for BeOH(g)[1], the ΔH°_{f298} and S°_{298} for BeOH(g) are found to be -46.8 $\pm$ 3.8 kcal/mole and 54.0 $\pm$ 1.7 cal/deg/mole, respectively. The corresponding average 3rd Law value for the heat of reaction, $\Delta H_{r2235^\circ K}$, is 87.2 $\pm$ 0.5 kcal. The free energy and heat of reaction for the 24 experiments are listed in Table IV. The Third Law ΔH_{f298} for BeOH(g) is calculated as -48.2 $\pm$ 0.5 kcal/mole. The entropy of BeOH(g) listed in the JANAF Tables is 53.29 cal/deg/mole. A summary of the thermodynamic functions for BeOH(g) is presented in Table V.

D. Summary

The excellent Second and Third Law agreement, supported by the experiments performed employing a mixture of hydrogen and water, establish the validity of the reaction of BeO with H_2 to produce BeOH. The recommended values for heat of formation and entropy of BeOH(g) at 298°K are -47.0 $\pm$ 2 kcal/mole and 54.0 $\pm$ 1 cal/deg/mole respectively.

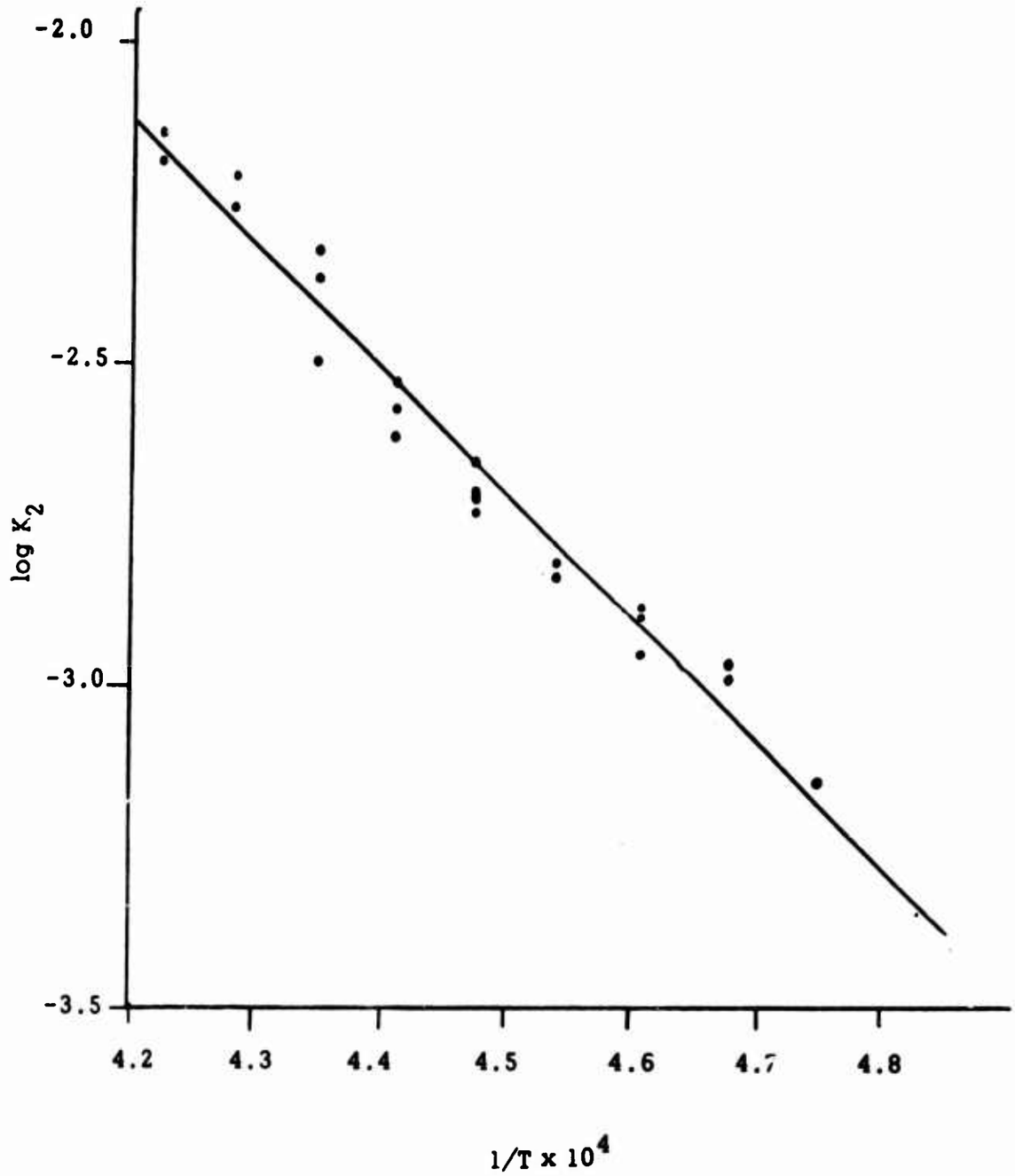

Fig. 3 The Log of the Equilibrium Constant for the Reaction
$BeO(c) + 1/2H_2(g) = Be(OH)(g)$
As a Function of the Reciprocal Temperature

III. THERMODYNAMIC PROPERTIES OF $AlCl_2$ AND Al_2Cl_4

A. Introduction

Several values have been published in the JANAF Tables for the heat of formation of AlCl as a result of the reaction

$$AlCl_3(g) + 2Al(l) = 3AlCl(g) \qquad (1)$$

which has been studied by means of transpiration experiments. A recent study of this reaction in this laboratory[12] by means of molecular flow effusion has essentially confirmed these values. No data appears in the published literature for either $AlCl_2$ or its dimer Al_2Cl_4. On the assumption made in the JANAF tables that the heat of reaction for

$$AlCl_3(g) + AlCl(g) = 2AlCl_2(g) \qquad (2)$$

would be essentially zero, a value for ΔH_{f298} for $AlCl_2$ has been estimated as -75 ± 20 kcal/mole. Based on this estimate it would appear that a high percentage of $AlCl_2$ would be produced in a reaction of aluminum chloride vapor and aluminum in the temperature range from 700 to 1,000°K. Also, if the heat of dimerization

$$2AlCl_2(g) = Al_2Cl_4(g) \qquad (3)$$

were approximately 50 kcal a considerable amount of the dimer would also be present in this same temperature range. There is no table for $Al_2Cl_4(g)$ in the JANAF Tables.[1]

Therefore, in order to obtain thermal data for $AlCl_2$ and its dimer Al_2Cl_4 a number of transpiration experiments were performed at atmospheric pressure in the temperature range 800 to 1000°K. These experiments involved the use of argon as the carrier gas for aluminum chloride vapor and was passed over pure aluminum, both solid and liquid.

B. Experimental

1. Apparatus

The experimental apparatus employed in this study consisted of a dual heating system for: (1) generating aluminum chloride vapor, and (2) heating the cell containing aluminum to the desired transpiration temperature. A schematic diagram of the entire apparatus and a detailed diagram of the transpiration cell are shown in Figs. 4 and 5.

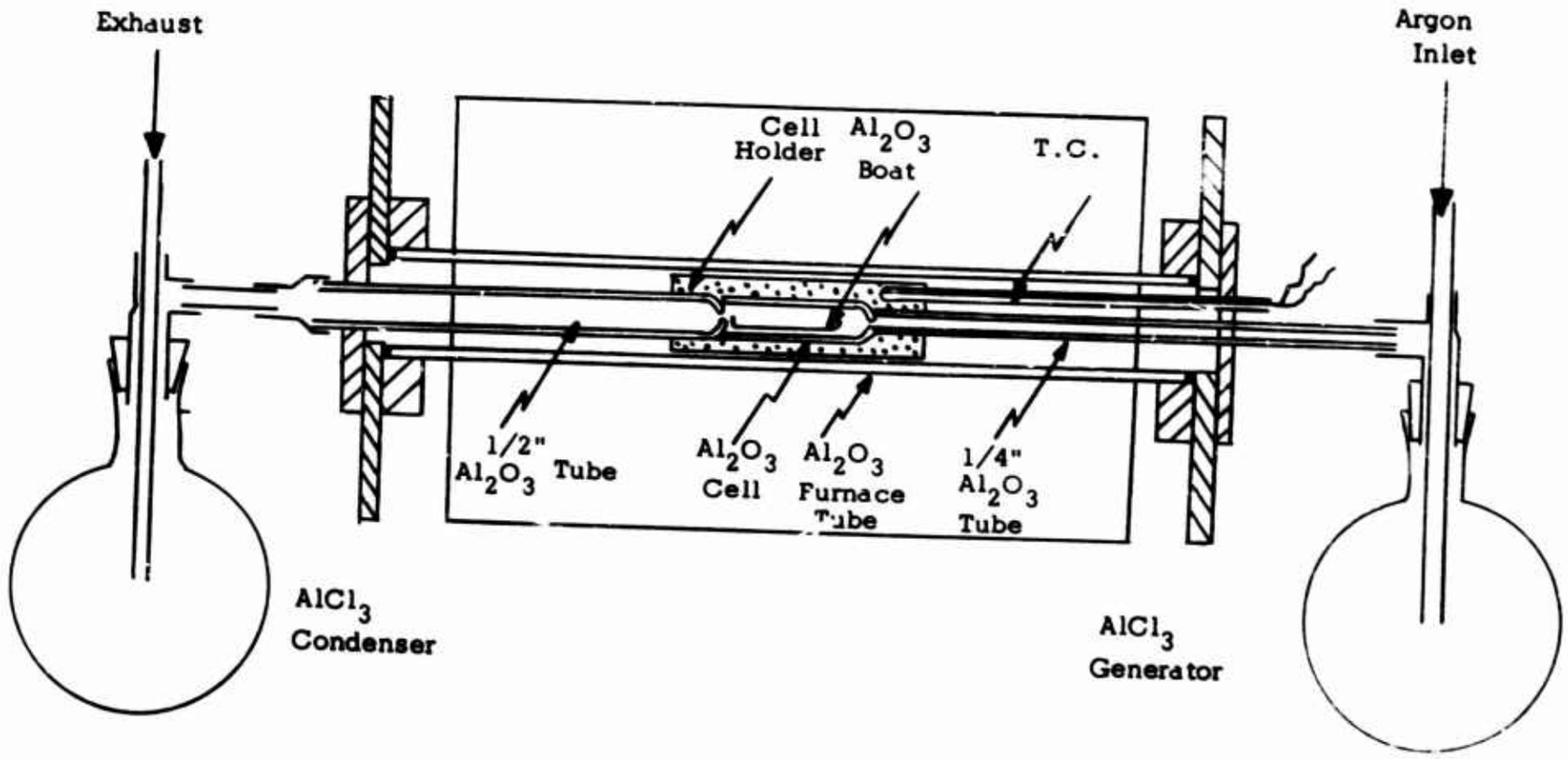

Fig. 4 Al - $AlCl_3$ Reaction System

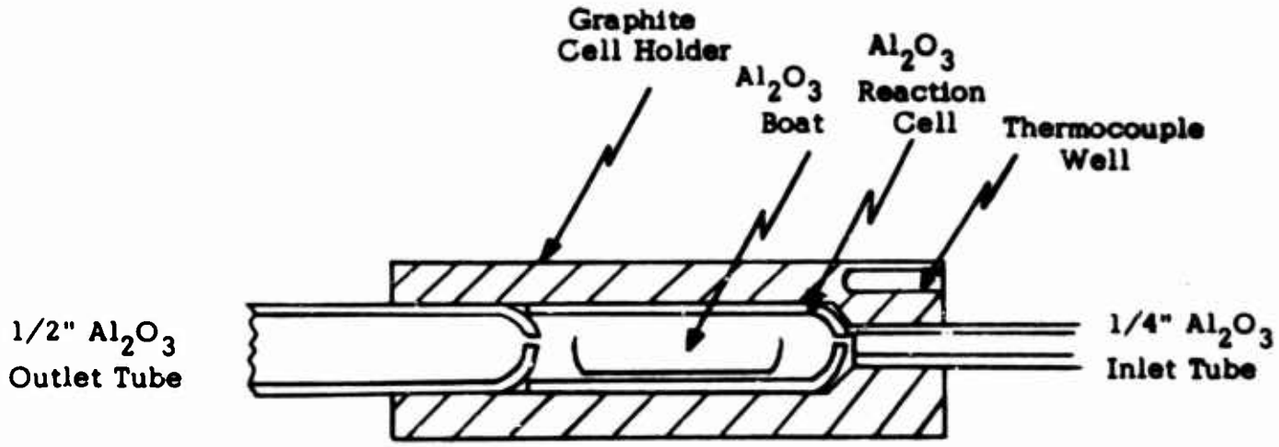

Fig. 5 Al - $AlCl_3$ Reaction Cell Assembly

The gaseous aluminum chloride was generated by heating the highly purified $AlCl_3(c)$ in a 250 ml glass flask by means of a heating mantle. A saturable core reactor-recorder combination was used to monitor and control the temperature of the flask. The flow rate of the gaseous $AlCl_3$ was controlled by controlling the temperature of the $AlCl_3$ generator. The flow rate of high purity argon was adjusted and measured employing very fine metering valves and an accurately calibrated flow meter and was used to carry the $AlCl_3$ into the reaction zone.

The furnace was a heavily insulated 12" long by 1-1/4" diameter nichrome resistance type. The furnace tube was constructed of aluminum oxide and measured " i.d. Each end of the furnace tube was closed by a monel flange, which also provided the openings for the gas delivery and exit tubes, as well as for the chromel-alumel thermocouple. The temperature of the cell was held constant by means of a silicon controlled rectifier-recorder combination.

The aluminum was contained in an aluminum oxide boat placed inside an aluminum oxide tube 10 mm i.d. The orifice and inlet hole of the reaction cell measured 1.5 mm in diameter, preventing any significant back diffusional losses in the reaction cell. The tube admitting the $AlCl_3$, argon mixture to the cell was also constructed of aluminum oxide.

The aluminum chloride in the argon-aluminum chloride vapor mixture was collected in a 250 ml flask after leaving the reaction zone. The aluminum chloride generator and collection flasks were connected to the transpiration apparatus with teflon and monel fittings. These fittings were heated with heating tapes and four immersion heaters were attached to the flanges in the ends of the furnace tube to prevent condensation of the aluminum chloride vapor entering or leaving the reaction zone. The temperature of these heating tapes and immersion heaters was maintained at approximately 230°C by the use of variable rheostats.

2. Procedure

The commerically obtained aluminum chloride (anhydrous) of 99.5% purity was further purified by sublimation prior to its use. The sublimation procedure also converted traces of moisture into HCl(g) which would be driven off as a vapor. As a further precaution against impurities, prior to each run approximately 1 gram of 99.9%, 200 mesh, aluminum powder was added to the sublimated aluminum chloride and thoroughly mixed by vigorous agitation for use in the generator flask.

The procedure employed for all experimental runs consisted of heating the sample of Al to the desired temperature under a stream of pure argon (99.998% purity). After the desired temperature was reached and automatic control established, the $AlCl_3$ boiler was heated rapidly to its predetermined temperature while argon was swept through it. At the desired temperature automatic control was established and the runs carried out for periods of 1-7 hours. Weight loss of the Al samples was established by weighing before and after each run. The amount of $AlCl_3$ passed over the sample was determined by weighing the generator before and after each run. After leaving the reaction the $AlCl_3$ in the gas mixture was collected in a second flask and weighed. (This weight gain was essentially equal to the weight loss in the first flask).

The weight loss of aluminum due to vaporization by passing argon alone over the aluminum sample was found to be insignificant and in agreement with that predicted from the published vapor pressure of aluminum. To further check that no HCl or water vapor was present in the aluminum chloride generator flask argon gas was passed through the generator, which was heated to 50°C, and then passed over a sample of aluminum in the reaction cell, which was heated to 900°K. At this low generator temperature the quantity of $AlCl_3$ in the vapor state is very small and therefore the resulting quantity of aluminum lost due to the reaction with $AlCl_3$ would also be insignificant. Thus any large losses of aluminum would have to be attributed to the entrained HCl(g) which reacts quantitatively with aluminum at the experimental temperatures. Since no reaction was observed it can be concluded that the reaction taking place is due to $AlCl_3$ and not to impurities.

C. Discussion

The obtaining of the requisite thermal data required an analysis of a series of 33 transpiration experiments in the temperature range of 800 to 1000°K and at 25° temperature intervals. The flow rates were in the range 15 to 25 cc/min which were sufficient to establish equilibrium of the vapor species above the aluminum. The orifice in the cell prevented any appreciable back diffusion. The experimental data including $AlCl_3$ and Al weight losses and flow rates are presented in Table VI.

Four transpiration studies[13,14,15,16] and a spectrographic study[17] gave results of the heat of reaction (1) in good agreement with those of the effusion experiments previously performed in this laboratory[12] for the reaction in the temperature range 930 - 1034°K. The equilibrium constants obtained from the

effusion data were chosen as the basis of correcting the total weight loss of Al for this reaction, since at low pressure $\sim 10^{-5}$ atm., the dissociation of higher chlorides to AlCl would be more likely. Also, the dimerization equilibrium

$$Al_2Cl_6(g) = 2AlCl_3(g) \qquad (4)$$

was employed in correcting the $AlCl_3$ flow data.

The remainder of the Al weight loss could then be distributed between $AlCl_2$ and its dimer Al_2Cl_4. The appropriate reactions would be

$$2AlCl_3(g) + Al(l,s) = 3AlCl_2(g) \qquad (5)$$

and

$$4AlCl_3(g) + 2Al(l,s) = 3Al_2Cl_4(g) \qquad (6)$$

The partial pressures involved for the necessary equilibria were calculated from the weight loss data by means of the gas law equation,

$$P = \frac{nRT_o}{V_o} \qquad (7)$$

where n is the number of moles of the specie formed from liquid or solid Al reaction in unit time with a given volume V_o of transpiring gas at a pressure of one atmosphere.

This gas includes all species, i.e., A, $AlCl_3(g)$, $Al_2Cl_6(g)$ and the products formed. T_o : the ambient temperature. Thus the partial pressure of AlCl in atmospheres would be

$$P_{AlCl} = \frac{n_{AlCl}}{n_T} \qquad (8)$$

where n_T is the total moles of gas in the transpiration mixture. A preliminary plot of the equilibrium constant for reaction (6) vs 1/T based on the assumption that reaction (5) was negligible showed extreme curvature indicating a possible mixture of the two species $AlCl_2$ and Al_2Cl_4. (See Fig. 6) Therefore, an iterative process was adopted for the solution of equations (5) and (6). After calculating a partial

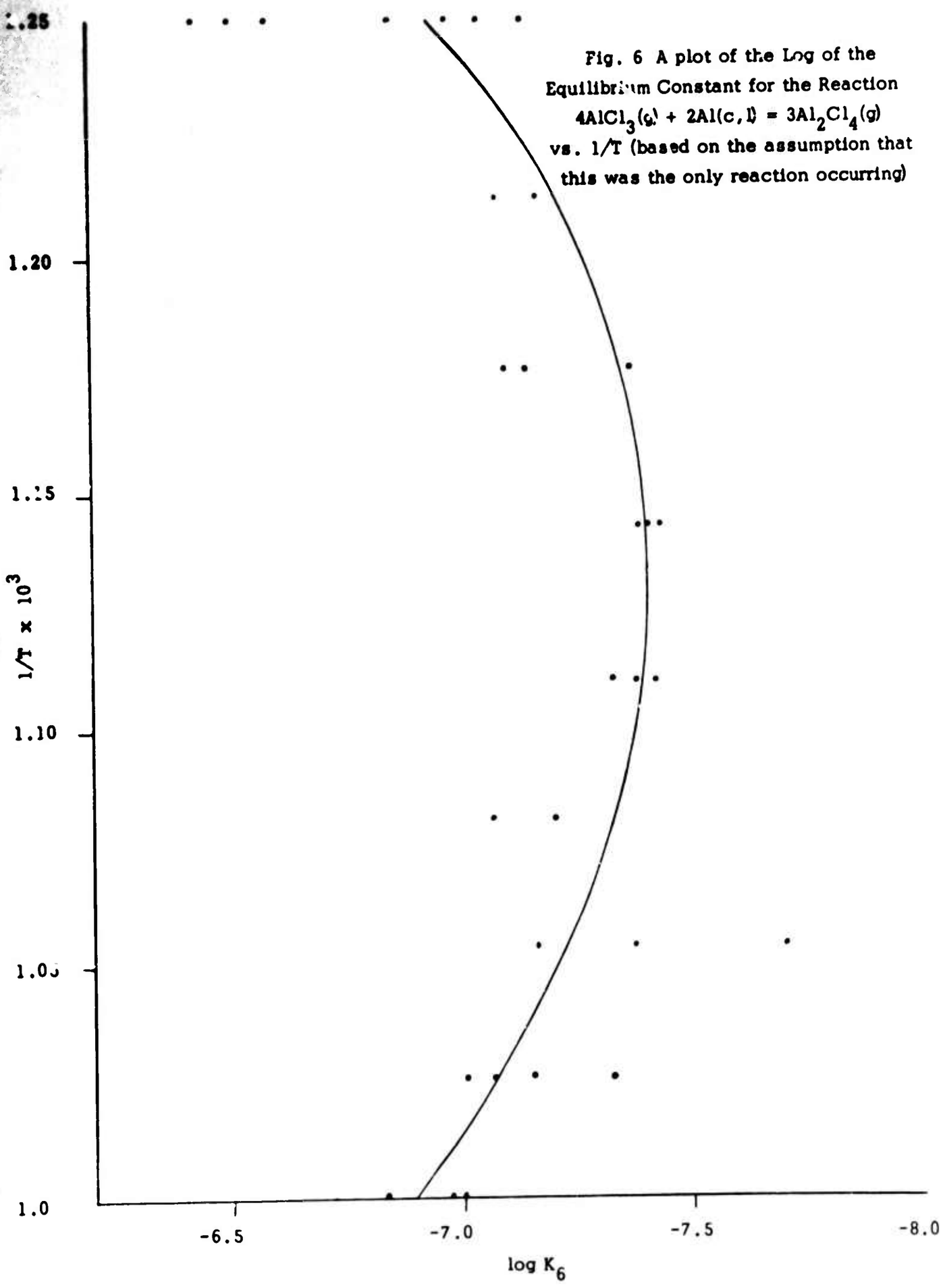

Fig. 6 A plot of the Log of the Equilibrium Constant for the Reaction $4AlCl_3(g) + 2Al(c,l) = 3Al_2Cl_4(g)$ vs. 1/T (based on the assumption that this was the only reaction occurring)

pressure of the AlCl(g) from equation (1) to obtain a weight loss attributed to reaction (1), the remainder of the weight loss was distributed by means of an interative procedure between both $AlCl_2$ and Al_2Cl_4.

The iteration was based on the assumption that for the proper distribution of weight loss between the two species straight lines would occur for the slopes representing the ΔH_r for the reactions represented by equations (5) and (6).

The iteration was begun with the assumption that the entropy listed in the JANAF Tables[1] for the triatomic molecule $AlCl_2$ was sufficiently accurate (within 3 eu) to allow free energy calculations for reaction (5), based on assumed values for the heat of formation of $AlCl_2(g)$. After each iteration corrections were made for the Al weight loss due to $AlCl_2$ and the free energy for reaction (6) was calculated.

Table VII presents the partial pressures and weight losses calculated for the species involved in the various equilibria. The equilibrium constants K_1 for reaction (1) are from the effusion experiments[12]. K_4 represents the equilibrium constant for the dimerization reaction (4) and are taken from the JANAF Tables[1]. K_5 is the equilibrium constant for reaction (5) based on a value -66 kcal/mole for ΔH_f $AlCl_2(g)$ at 298°K and on specific heats and entropies from the JANAF Tables[1]. Finally, K_6 is the equilibrium constant for reaction (6) after corrections were completed for reactions (1) and (5).

A fairly straight slope was obtained for reaction (6) (see Fig. 7) based on an assumed value of -66 ± 1 kcal for ΔH_{f298} for $AlCl_2(g)$. The ΔH_r and ΔS_r of reaction (6) were found to be -25.9 ± 2.9 kcal and -64.2 ± 3 cal/deg/mole respectively at 900°K. This yields values of -194.8 ± 1.0 kcal/mole and 115.7 ± 1.1 cal/deg/mole for ΔH_{f900} and S°_{900} for $Al_2Cl_4(g)$. A corresponding third law heat of reaction could not be calculated since no value for the entropy of $Al_2Cl_4(g)$ is reported. However, the second law entropy of 116 cal/deg/mole is a reasonable value for a molecule of this size and structure and may be compared to the estimated value of 115 cal/deg/mole (with an uncertainty of 5 e.u.) for $B_2Cl_4(g)$ listed in the JANAF Tables.[1]

Since heat capacities have not been estimated for $Al_2Cl_4(g)$ calculations of the heat of formation and entropy at 298°K are speculative. However, a value for ΔH_{f298} of -194 ± 5 kcal/mole and S°_{298} of 90 ± 5 cal/deg/mole are considered reliable.

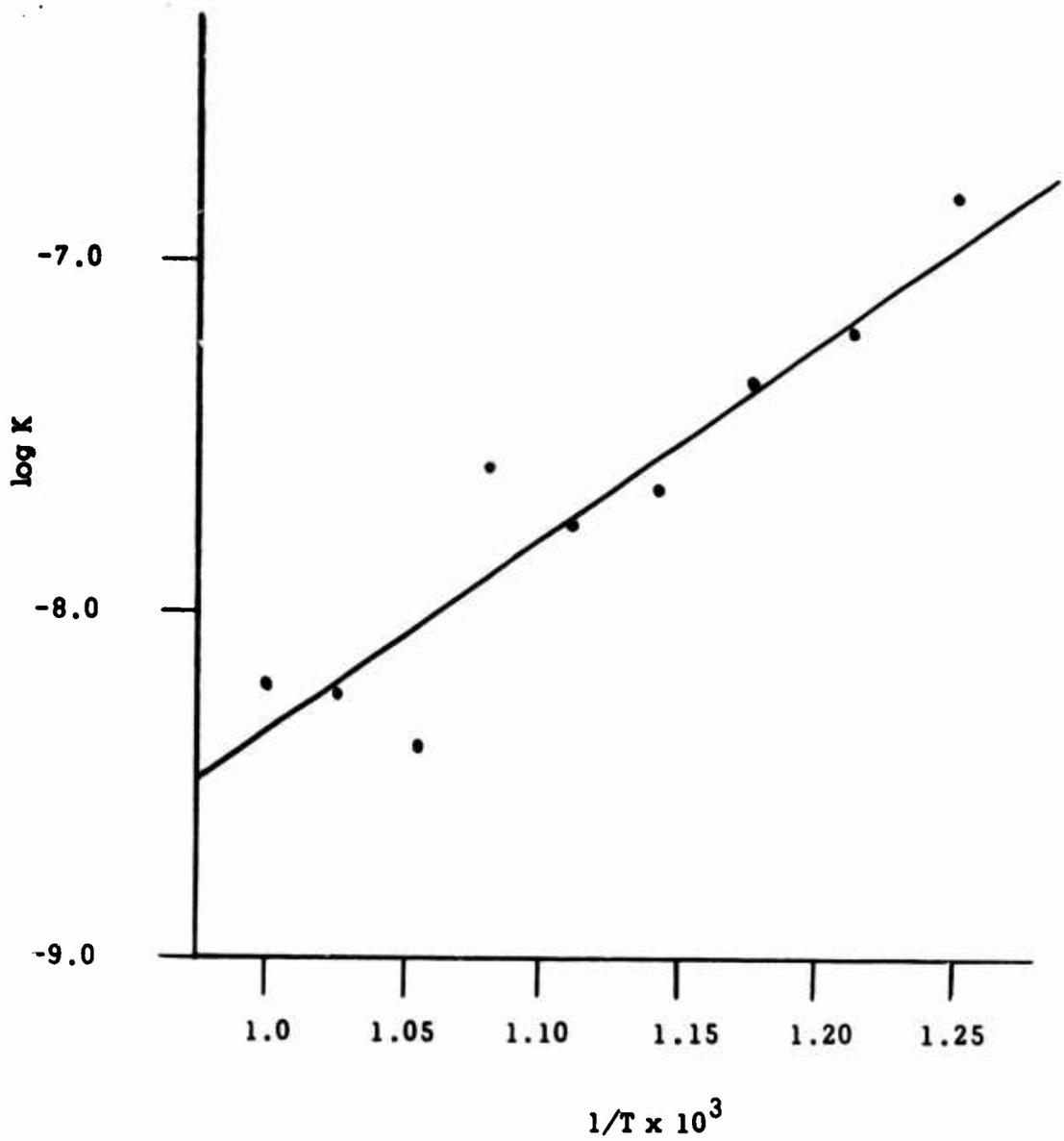

Fig. 7 The Log of the Equilibrium Constant for the Reaction
$Al(c,l) + 4AlCl_3(g) = 3Al_2Cl_4(g)$
As a Function of the Reciprocal Temperature

The heats and entropy of dimerization for reaction (3) are -62 kcal and -47 cal/deg/mole at 298°K, respectively. This compares to dimerization values for B_2Cl_4 of -77 kcal and -44 cal/deg/mole for the heat and entropy respectively. The thermodynamic functions for $AlCl_2(g)$ and $Al_2Cl_4(g)$ are presented in Table VIII.

Having obtained a fairly accurate value for ΔH_f of $AlCl_2$ it was possible to obtain a check on the assumption of equation (1) for the effusion data. In the temperature range of the effusion experiments[12] for reaction (1) a ΔH_r of 95 kcal/mole was obtained. Employing a value of -66 kcal/mole for ΔH_{f298} of $AlCl_2(g)$ a ΔH_r at an average temperature of 900°K for reaction (5) of 86 kcal is calculated. Since the slopes for equations (1) and (5) differ by only 9 kcal or 10%, curvature in reaction (1) would not be readily seen unless reaction (5) were contributing more than 10% to the Al weight loss. Therefore, in order to check the validity of the effusion experiments in the temperature range 850°K to 1000°K free energies (extrapolated from previous results at this laboratory[12]) were calculated for equation (2) at the highest and lowest temperatures, 850°K and 1000°K. The calculations are presented in Table IX. Since the amounts of $AlCl_2(g)$ in equilibrium with AlCl and $AlCl_3$ range from only 5 to 8% over this temperature range the validity of the effusion experiments are further established. However, it would appear that at atmospheric pressure transpiration experiments would involve considerable quantities of both AlCl and $AlCl_2$.

D. Summary

An analysis of the effusion and the transpiration experiments to obtain thermal data for AlCl(g), $AlCl_2(g)$ and $Al_2Cl_4(g)$ shows that they are self-consistent. Thus, the recommended values for ΔH_{f298} for $AlCl_2(g)$ and $Al_2Cl_4(g)$ are -66 ± 3 and -194 ± 5 kcal/mole respectively. The recommended entropy S°_{298} of $Al_2Cl_4(g)$ is 90 ± 5 cal/deg/ mole.

IV. THERMODYNAMIC PROPERTIES OF HBO(g)

A. Introduction

Ion intensities have been reported for the specie HBO(g) in mass spectrometric studies[18] involving B_2O_3 and $H_2O(g)$. However, no thermal data have been published. The current JANAF Tables[1] report an estimated value of -20 ± 20 kcal/mole while the previous gray Tables[3] reported a value of -47 ± 15 kcal/mole based on a National Bureau of Standards estimate.

A mass spectrometric study over the temperature range 1160 - 1405°K has been made for the reaction of $B_2O_3(l)$ and $D_2(g)$ to obtain a heat of formation of the high temperature stable specie DBO. Initial experiments were performed on the reaction of B_2O_3 with H_2 which indicated the formation of HBO; however, the accuracy of the mass spectrometer intensities was impaired by the high background at mass 28, where the background intensity was 30 times larger than the background of mass 29. Since most compounds of deuterium have heats of formation nearly equal (within 1 kcal) of those of hydrogen it became apparent that a more precise value for HBO could be obtained by employing deuterium.

B. Experimental

The experimental procedure employed for the studies combines a high vacuum high temperature apparatus together with a quadrupole mass spectrometer. The vacuum furnace is similar to the one used for the BeOH experiments.

A graphite furnace mounted in a high vacuum chamber was constructed and tested for the purposes of this investigation. The furnace is capable of maintaining temperatures in excess of 2300°K, for long periods of time. A high vacuum system is necessary to keep the background or residual gas pressure low enough to obtain high sensitivities of the species produced. The vacuum system employed in the apparatus was capable of providing, with the aid of a cold trap, a vacuum of better than 1×10^{-7} mm Hg, at a cell temperature of 1800°K in the furnace, while at room temperature the pressure was 2×10^{-8} mm Hg.

Details of the various components of the experimental apparatus and their operating procedures are described in the following section.

1. Apparatus

a. Vacuum System

The furnace chamber was fabricated in a cross configuration using 304L stainless steel 8" and 4" schedule 10 pipe and 3/8" thick plate. All seams were heli-arc welded on the inside to minimize the outgassing load.

The quadrupole mass spectrometer probe was mounted on one of the 8" pipe plate flanges. The other 8" flange supported the furnace assembly, which is described in the following section. The cross was attached to the vacuum pump via one of the 4" branches while the other was sealed by a plate flange containing a 2" quartz window for visual temperature measurement. Only viton O-rings or teflon gaskets have been used for seals throughout the entire system. The cross section drawing of the chamber may be seen in Fig. 8 and photographs of the assembly are shown in Figs. 9 & 10.

During furnace operation, the 8" pipe was cooled with freon which was passed through a coil of 3/8" copper tubing soldered to the outside diameter of the cross while each plate flange of the 8" pipe was air cooled using high capacity blowers.

The furnace chamber was evacuated by a 4" high speed NRC diffusion pump (750 l/sec), charged with Dow Corning 705 oil. The diffusion pump is backed by a Welch Duo-Seal two stage fore pump (100 l/min). The back streaming of the oil vapor was essentially eliminated by the water cooled cap of the diffusion pump and the inclusion in the system of a NRC expanded water cooled chevron baffle. A 4" thimble cold trap was included in the system.

b. Furnace

The heating element of the furnace consisted of twelve 6" long x 1/8" o.d. high density graphite rods (resistivity 1500 x 10^{-6} ohm cm^{-1}) arranged in series and had a resistance of 2.9 ohms at 20°C. The rods were held 0.386" apart between centers in 1/4" o.d. graphite couplers. This distance is equivalent to a 30° chord of a 1.491" diameter circle. The heater rods were kept parallel to one another by additional 1/8" o.d. graphite rods placed in the center of each coupler. These support rods passed through 1/4" holes in the end shields and were capped at the ends with alumina tubes closed at one end (1/4" o.d. x 1/8" i.d. x 1" long). This arrangement allowed the positioning of the graphite support rods accurately in the end shields and the overall result was an extremely rigid furnace element. Figure 11 shows in detail the coupling arrangement between two graphite rods while in Fig. 12 the support rod relationship to the heater element and alumina spacer can be seen.

Six five mil tantalum cylinders, 2-1/2" to 5" in diameter were used as the radiation shields. The lengths of the shields began at 8" and increased in 1/2" increments to 10-1/2" so that with the end shields in place

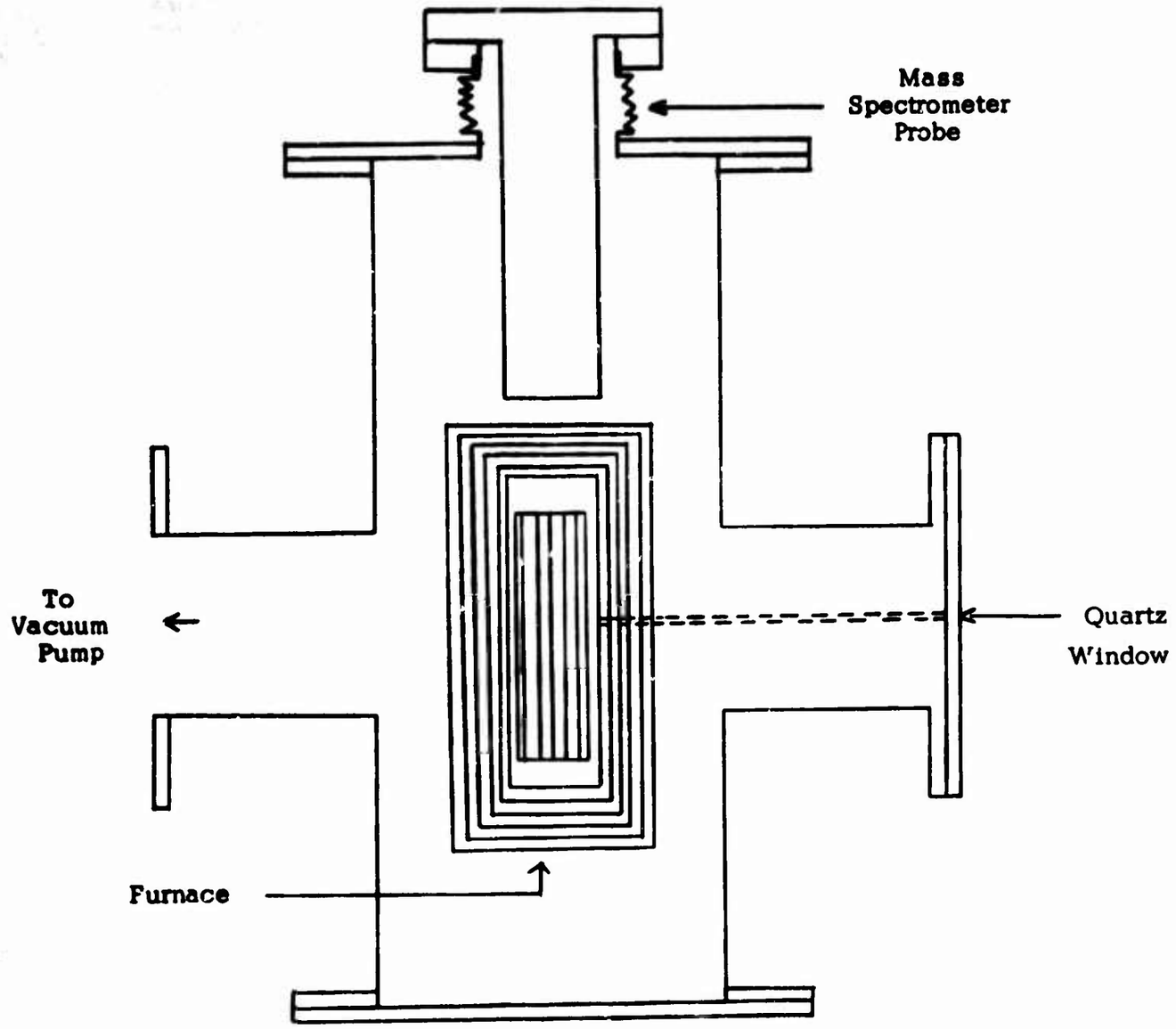

Fig. 8 Furnace Chamber

Fig. 9. Mass Spectrometer and the 4 Inch Vacuum System.

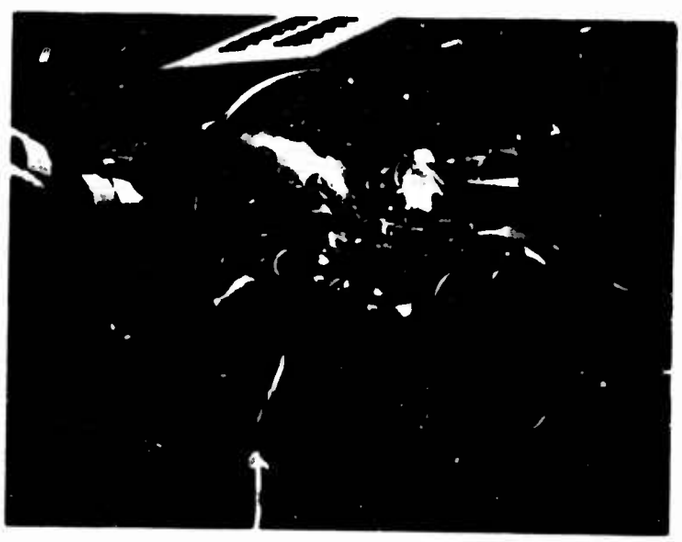

Fig. 10. Furnace Port. The Reaction Cell and Flow System Sub-Assembly in Center.

Fig. 11. Close Up View of Graphite Coupler used in Furnace Element

Fig. 12. View Showing Alignment Rod With Alumina Insulator

the shields were a set of nested cylinders 1/4" apart. Tantalum rods 1/8" diameter, spaced 120° apart around both ends, and 1/4" o.d. x 0.245" long graphite spacers kept the shields concentric and rigid. These tantalum rods were bolted to three 1/4" o.d. stainless steel rods which supported the shield system 4" off the flange plate. Fig. 13 shows a top view of the shields with the furnace element in place. The complete furnace assembly is shown in Fig. 14.

In each of the top end radiation shields, there was a 1/2" hole which was coaxial with the mass spectrometer quadrupole analyzer. The cylindrical shields contained a set of 1/4" holes which were coaxial with the viewing port on the vacuum chamber. This hole provided a reasonable approximation to a black body cavity for visual temperature measurement.

c. Temperature Measurement and Control

The temperature was monitored by a tungsten-5% rhenium versus tungsten-26% rhenium thermocouple, mounted in the furnace just outside the heating zone. The thermocouple was calibrated against a 0.1% platinum versus platinum-10% Rhodium thermocouple at 30° intervals over the temperature range of the study. The tungsten-rhenium thermocouple was measured on a Leeds and Northrup K-3 potentiometer.

The K-3 bridge was set at the desired voltage and the imbalance plotted on a Leeds and Northrup Speedomax W recording potentiometer (center zero, 1 mV full scale). The control current to the 100 amp 230 volt Fincor SCR power supply was fed from a Leeds and Northrup Series 60 current adjusting type control system, acting on the information from the recording potentiometer. The sensitivity of the control loop at 1400°K. was about 0.1 to 0.2°C.

d. Reaction Cell and Flow System

The reaction cell and flow system were mounted on a separate plate which was sealed to the main flange plate via an O-ring. This arrangement (as seen in Fig. 15) facilitates the maintenance of the reaction system without disturbing the furnace assembly. A 1" hole in each of the bottom end shields permitted the assembly to pass into the furnace. Mounted on the 1/4" o.d. by 0.010" wall tantalum flow tube was a set of 5 mil tantalum 1" discs which sealed the hole in the radiation shields.

The reaction cell, fabricated from platinum, was 5 cm long by 1.27 cm o.d. by 1.12 cm i.d. At the closed end of the cell an exit tube 2.5 cm long by .25 cm o.d. by 10 cm i.d. was welded. The molten B_2O_3 was held in a

Fig. 13. Top View of Furnace Shields with Furnace Element in Place

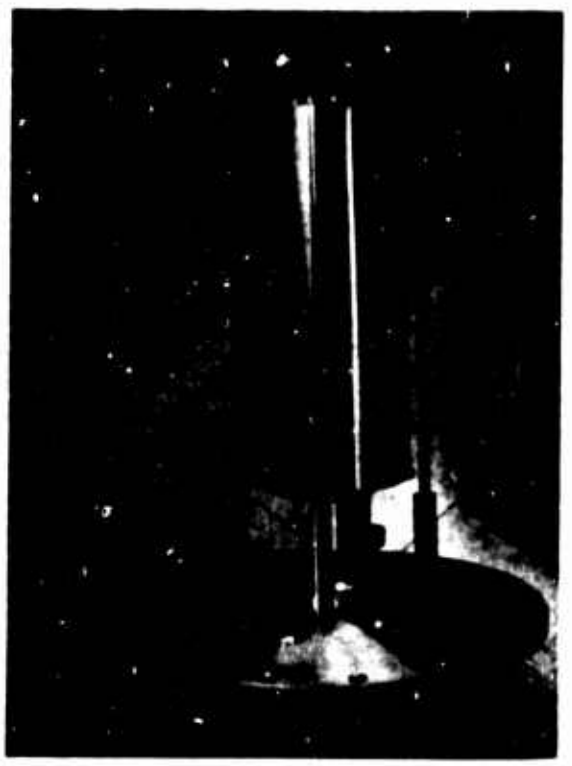

Fig. 14. Complete Furnace Assembly Mounted on 8" Plate Flange

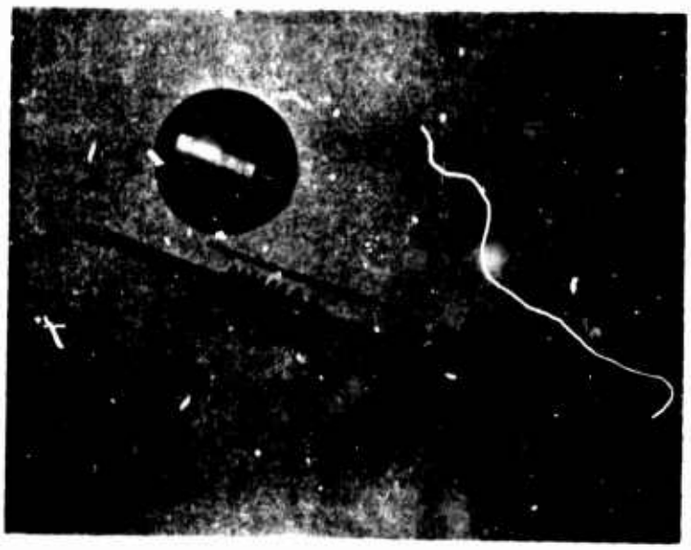

Fig. 15. View of Sample Port Assembly Showing Relationship of Flow Tube, Reaction Cell, Shields and Thermocouple

platinum boat 4.5 cm long and 0.5 cm deep. The reaction cell was joined to the 1/4 inch o.d. by 230 inch i.d. tantalum flow tube via a tantalum holder. The i.d. of the holder was machined .003" larger than the o.d. of the cell to allow 1 mil platinum foil to be placed around the cell and inserted into the holder for a distance of 1/8". The closeness of fit allowed moderately high pressures of D_2 gas to be used (e.g. 10mm) if desired.

The D_2 gas was fed to the cell from a two liter reservoir initially filled to a pressure of 0.1 atm via a Granville Phillips variable leak. Based on the Knudsen equation, the flow of D_2 gas through the orifice of the platinum cell at 1400°K and 10^{-4} atm. is approximately 2.0 cc hr^{-1} at STP. Thus after one hour only a negligible change (1%) in the cell pressure occurs. The gas pressure was measured by a Veeco Dv-1 thermocouple gauge, calibrated for D_2 gas.

e. Quadrupole Mass Spectrometer

The quadrupole mass spectrometer used in this study, Model QUAD 200 (manufactured by Electronic Associates, Inc.) facilitates its installation in small vacuum systems, without sacrificing loss in sensitivity and resolution. This instrument has a resolution of 500 and a sensitivity of 10^{-14} to 10^{-15} torr for N_2, when an electron multiplier is used in conjunction with an electrometer amplifier. The quadrupole probe, factory mounted on a 4" Ultek flange, projects approximately 9" into the vacuum system (Figs. 16 & 17). The probe can be accurately aligned with the molecular beam from the reaction cell by sighting down the flow tube and adjusting the angle of the mass spectrometer with respect to the flange via a 3-1/2" i.d. bellows. The molecular beam can be intercepted to distinguish it from background by rotating a tantalum sector directly in front of the furnace slits (Fig. 18). The vacuum seal used for the rotating shaft is a simple Swagelock device using a teflon front ferrule as the seal. There was no detectible air leak during rotation.

C. Discussion of Results

The intensities of the four principal species, D_2O, DBO, DOBO and B_2O_3 were measured with the quadrupole mass spectrometer at a series of temperatures covering a range of 250°K (1160-1405°K). Twelve series of experiments were made encompassing a fifteen-fold change in the D_2 pressure (18-240 μ).

For the prime purpose of obtaining the heat of formation of DBO, only

Fig. 16. Quadrupole Probe

Fig. 17. Probe Mounted on Flange

Fig. 18. Alignment Device with Shutters

the following three reactions were considered.

$$D_2(g) + B_2O_3(l) = DBO(g) + DOBO(g) \qquad (1)$$

$$K_1 = (^{I}DBO)\ (^{I}DOBO)$$

$$D_2O(g) + B_2O_3(l) = 2DOBO(g) \qquad (2)$$

$$K_2 = \frac{(^{I}DOBO)^2}{(^{I}D_2O)}$$

$$B_2O_3(l) = B_2O_3(g) \qquad (3)$$

$$K_3 = {}^{I}B_2O_3$$

Since the $D_2(g)$ was maintained at a constant pressure its intensity was not included in K_1. This assumption is not valid at the highest temperatures of the study where there is a significant decrease (> 5%) of the D_2 pressure in the cell due to reaction, therefore, these points have been ignored.

A typical set of data obtained during a run is given in Table X and the plots of the log K for reactions (1) through (3) as a function of 1/T are shown in Fig. 19. Ion intensities for species obtained at higher temperatures are shown in Table XI for a pressure of 240 μ and at a temperature of 1518°K.

The mass spectra measurements were all made at an electron energy of 70 volts and an emission current of 1 ma. A study was also made at 16 volts electron energy and 1 ma emission current at 75 μ D_2 pressure, but the data for reactions (1), (2) and (3) were essentially equal to those at 70 volts (deviation in the slope of less than 2 kcal) indicating no significant contribution of fragment species to the major peak intensities. Table XII summarizes the data obtained from nine determinations on reactions (1), (2) and (3). The heats of reaction were derived from least squares treatment of the data.

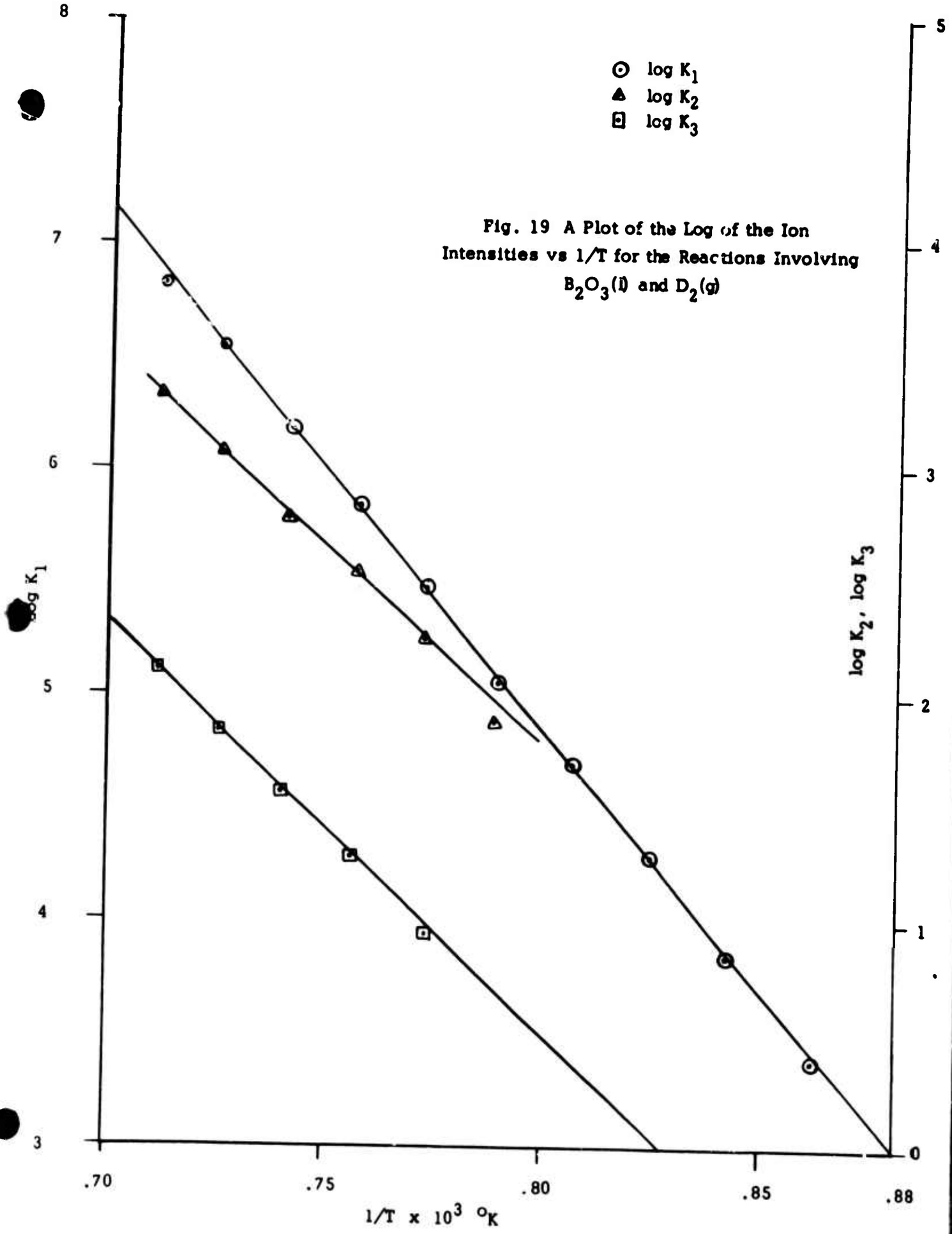

Fig. 19 A Plot of the Log of the Ion Intensities vs 1/T for the Reactions Involving $B_2O_3(l)$ and $D_2(g)$

1. ΔH_v of $B_2O_3(l)$

The six runs obtained in this study agree with one another within $\pm$ 2 kcal/mole. The average value for the second law ΔH^o_v at the mean temperature of 1320°K is 86.3 kcal/mole with an average deviation of $\pm$ 1.5 kcal/mole. This value is in good agreement with most of the determinations. However, Buchler and Berkowitz-Mattuck[19] report 93.6 $\pm$ 3 kcal/mole at 1300°K by mass spectrometry and Hildenbrand, Hall and Potter[20] 93.3 $\pm$ 2 at 1500°K by Knudsen vapor pressure measurements.

The reduction of ΔH^o_{v1320} to 298°K gives 93.6 $\pm$ 2 kcal/mole. This value compares favorably with 95.2 $\pm$ 09 obtained by M.D. Sheer[21]; 90.5 $\pm$ 1.5 from mass spectra measurements of White, Walsh, Goldstein and Dever[22]; 93.1 $\pm$ 0.7 given by Sommer[23]; 92.8 $\pm$ 1.4 obtained by Blackburn[24]. Margrave in a recent article[25] questions the validity of the current JANAF Table of $B_2O_3(g)$ since he calculates 92 $\pm$ 3 kcal/mole for ΔH_{v298}. His third law ΔH_{v298} is 104 kcal/mole, which is in serious disagreement.

2. ΔH^o_r of $B_2O_3(l) + D_2O(g) = 2DOBO(g)$

The data obtained for this reaction was reproducible for the six series. The average value for the second law ΔH_{1320} is 81.5 kcal/mole with an average deviation $\pm$ 1.5 kcal/mole. This value is in excellent agreement with the mass spectra data of Meschi, Chupka and Berkowitz[26]. They reported 84.6 $\pm$ 4 kcal/mole for the ΔH_{1250} of reaction (2). White, Mann, Walsh and Sommer[27] obtained 78 $\pm$ 5 kcal/mole from the variation of the 2030 cm^{-1} band intensity of HOBO with temperature. Farber et al.[28] from measurements by the effusion method reported 80.8 $\pm$ 1.2 kcal/mole. The resultant ΔH_{f1320} of HOBO(g) is -135.9 $\pm$ 2 kcal/mole which reduces at 298°K to -133.5 $\pm$ 2 kcal/mole.

3. ΔH^o_f of DBO(g)

The data on reaction (1) gives an average second law ΔH^o_f at 1260°K for DBO(g) of -52 $\pm$ 3 kcal/mole and for HBO(g), -51 $\pm$ 3 kcal/mole. The high pressure runs at 240 μ D_2 pressure were discarded. The reduction of ΔH^o_f to 298°K for DBO(g) with the JANAF data gives -50.8 kcal/mole. Since the ΔH^o_f for most deuterium compounds is about 1 kcal/mole more negative, the ΔH^o_{f298} for HBO(g) is assigned a value of -50 $\pm$ 3 kcal/mole.

The JANAF[1] estimate of -20 kcal/mole for ΔH_{f298} is in serious disagreement with this experimental measurement; however, the previous estimate by W. H. Evans of -47 kcal/mole reported in the earlier Iterim JANAF Table[3] is in remarkable agreement with the value obtained in this study.

In order to obtain a second and third law correlation, the free energy of reaction

$$D_2(g) + B_2O_3(g) = DBO(g) + DOBO(g) \qquad (4)$$

at the temperature of 1400°K was combined with thermal functions of the reactants and products. The equilibrium constant for this reaction is approximately 0.2 within a factor of 5 at 1400°K. Since Margrave[25] had pointed out that a considerable discrepancy appears in the thermal functions for both liquid and gaseous B_2O_3, calculations were made with entropies listed in the latest JANAF Tables[1] and those in the earlier JANAF grey tables[29]. The entropy in the grey tables at 1400°K for $B_2O_3(g)$ is 92.9 e.u. while the value in the most recent JANAF Tables[1] is 99.5 e.u. Employing S_{1400} of $B_2O_3(g)$ of 92.9 cal/deg/mole a third law value of 17.3 kcal/mole for the heat of reaction (4) was obtained. This compares with 18.5 kcal/mole, for the average ΔH_r derived from the six experimental second law heat of reaction.

The ΔH_r which is obtained with the entropy value of 99.5 e.u. for $B_2O_3(g)$ yields a ΔH_r of only 8.1 kcal which is considerably lower than the second law value. Since Margrave also found a discrepancy of 12 kcal in the vaporization data of B_2O_3 between his second and third law values, it is likely that the JANAF entropy data for B_2O_3 is in error. The estimated entropies for HBO and HOBO may also be in error by as much as 2 to 3 entropy units (total) contributing from 3 to 4 kcal error in the ΔH_r.

V. THERMODYNAMIC PROPERTIES OF $Be(OH)_2(g)$

A. Introduction

The heat of formation of $Be(OH)_2(g)$ ($\Delta H^o_{f298} = -158.5 \pm 1.5$ kcal/mole) has been calculated from equilibrium data obtained from flow experiments performed by Grossweiner and Seifert[30] involving water vapor and crystalline beryllium oxide,

$$H_2O(g) + BeO(c) = Be(OH)_2(g) \qquad (1)$$

Young[31] in 1960 performed similar flow experiments and obtained a ΔF_{1673} of 27.7 kcal/mole for the free energy for reaction (1). This compared to Grossweiner and Seifert's value of 29 kcal/mole at the same temperature. Young's data resulted in ΔH^o_{f298} of -159.2 $\pm$ .7 kcal/mole for $Be(OH)_2(g)$. Regarding the entropy of $Be(OH)_2(g)$, the JANAF Thermochemical Tables[1] have estimated frequencies which yield an entropy (57.97 cal/deg/mole) in good agreement with these second law heats.

Recently, an extensive experimental program was conducted in these laboratories[5] which resulted in a second law value for ΔH_{f298} of 161 $\pm$ 7 kcal/mole for $Be(OH)_2(g)$ and a second law entropy at the average experimental temperature of 1705°K of 92.6 $\pm$ 4 cal/deg/mole. This compares with the entropy value from the JANAF Tables at 1705°K of 89.93 cal/deg/mole. Based on the JANAF entropy values, data of Blauer, et al,[5] yield an average third law $\Delta H^o_{f298^oK}$ of -165.9 $\pm$ 0.7 kcal/mole, a difference of nearly 5 kcal between the second and third law heats of formation.

In an effort to obtain more reliable entropy data for $Be(OH)_2(g)$ an experimental spectroscopic investigation was undertaken in these laboratories. Once spectra are obtained they can be resolved by means of statistical mechanics which provide the fundamental equations necessary for the evaluation of the entropy of a gas. These equations relate the energies of the various states - translational, rotational, vibrational and electronic - to the probability of their population under specified conditions.

Vibrational-rotational molecular spectra of polyatomic molecules normally appear in the near infrared. These spectra, when obtained with high-dispersion, high-resolution instruments, can be analyzed to provide the requisite data for entropy calculations.

The experimental program involved two important experimental considerations for the spectroscopic study which include: (1) an abundance of the species under study and (2) spectral resolution of these from spectra occurring from other species which may complicate the spectrum of the compound in question. The thermodynamics of the BeO-water vapor reaction are such that water will be present in the system, regardless of the method of generation of the $Be(OH)_2$. Therefore, the operating conditions under which $Be(OH)_2$ is generated must be chosen in such a manner that the $Be(OH)_2$ concentration is maximized and the H_2O is minimized.

An extrapolation of the data of Blauer et al[5] shows that 5% of $Be(OH)_2$ will be present in an equilibrium consisting of H_2O and $Be(OH)_2$ at 2500^oK.

The highest yield of $Be(OH)_2(g)$ is produced in the reaction of $H_2O(g)$ and BeO at high temperatures. Spectroscopic measurements may thus be made directly on this high temperature gas mixture or the specie may be trapped in a suitable matrix and the spectral data of this material may be obtained at cryogenic temperatures. Flame temperatures in excess of 2750^oK have been reported for the H_2-O_2 flame; therefore, this flame, producing water vapor at high temperature, was chosen for the production of the $Be(OH)_2$ specie.

B. Experimental

Since a high temperature flame is capable of providing the necessary spectral data, the experimental apparatus was constructed so that either absorption or emission measurements could be made. The burner assembly and housing were designed for mounting in the sample space of a Perkin-Elmer 421 dual grating infrared spectrometer.

Figure 20 is a cross-sectional view of the H_2-O_2 burner assembly and housing. Space limitations necessitated the inclusion of several mirrors to adapt the burner assembly light path to that of the spectrometer. For the absorption studies, light from the black-body radiator is deflected from the usual, straight-through path to a path which intercepts the flame and its products. In order to improve the amount of light reaching the infrared spectrometer (Perkin Elmer Infrared Grating Spectrograph Model 421) a collimated lens made from NaCl was placed at the exit of the light path from the apparatus. Photographs of the completed apparatus are shown in Figs. 21 and 22.

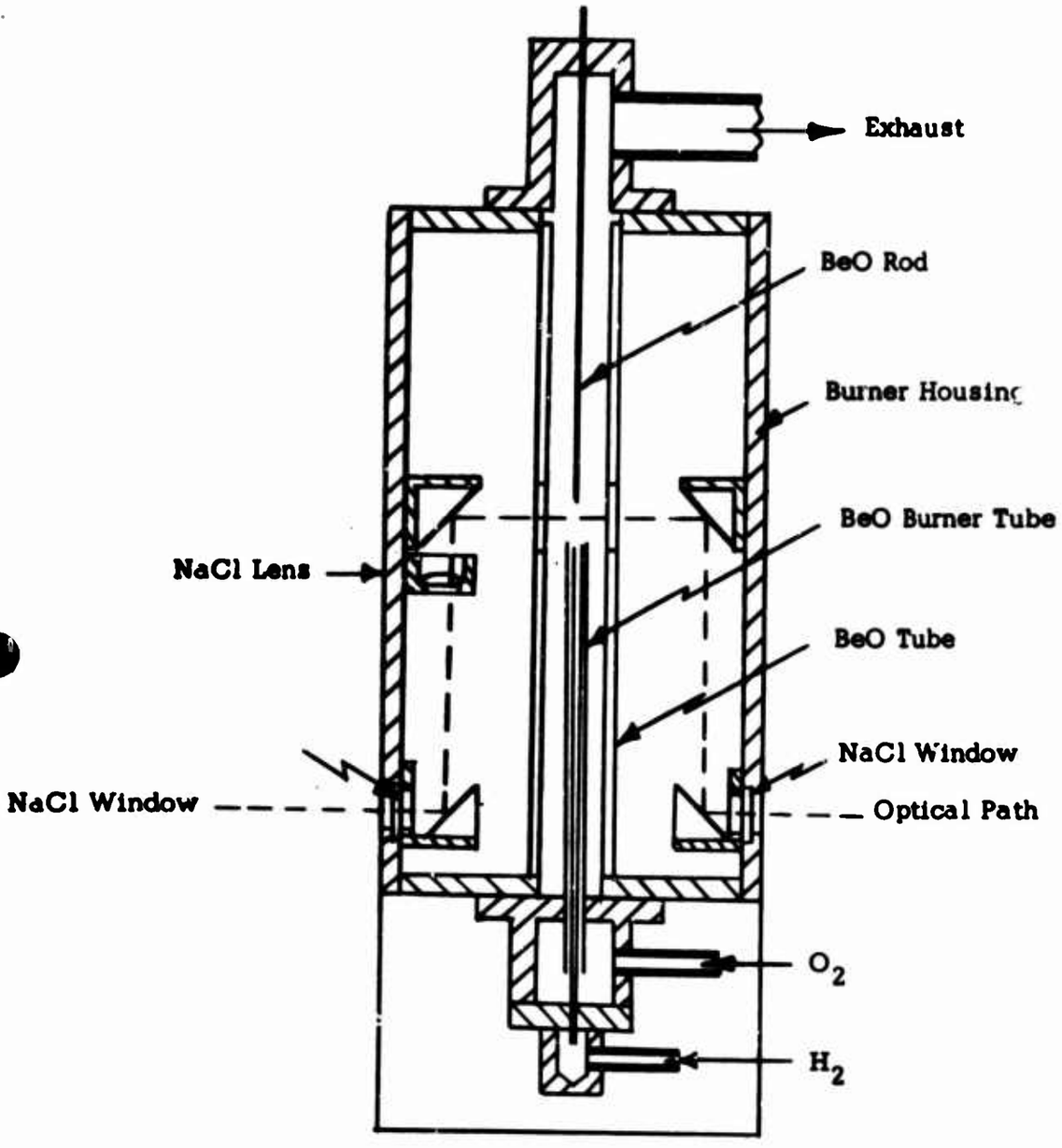

Fig. 20 Apparatus for $Be(OH)_2$ Generation

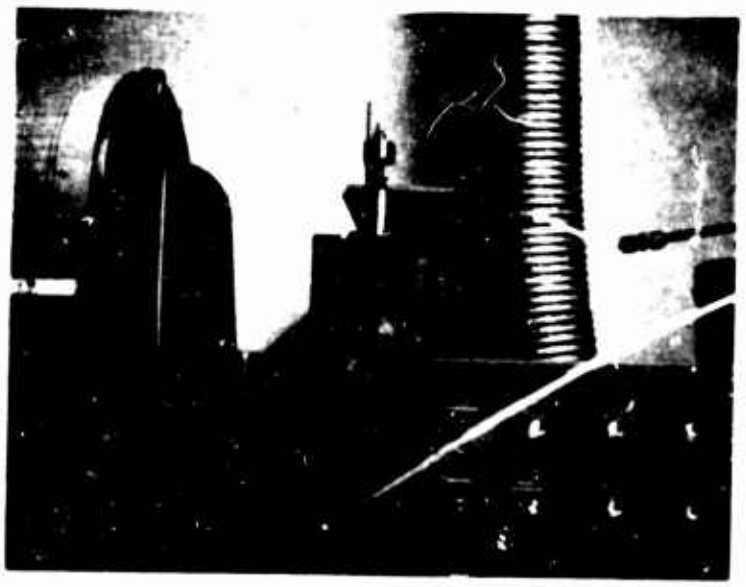

Fig.21. BeO-H_2-O_2 Emission Source Positioned in Spectrophotometer

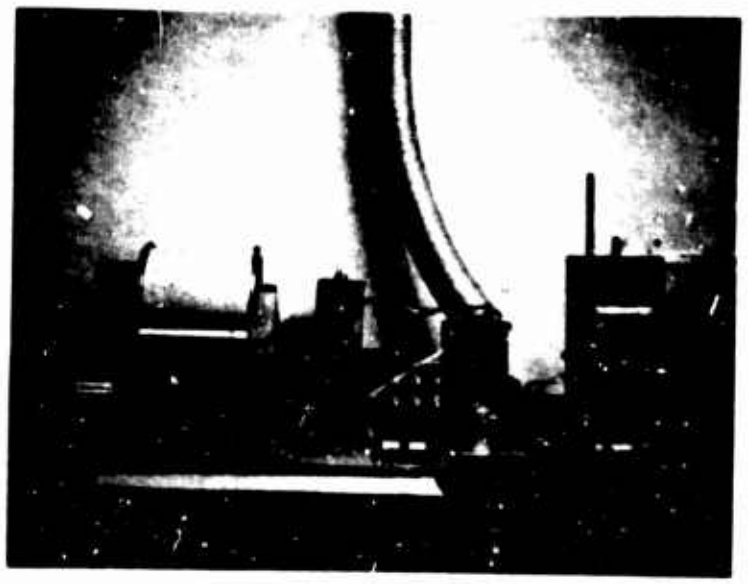

Fig.22. Complete Set Up for $Be(OH)_2$ Emission Studies

The primary site of the BeO-H_2O reaction is the inside wall of the oxygen-flow tube, above the end of the hydrogen tube, and a BeO target rod was inserted into the H_2-O_2 flame at this point. The burner tip was adjusted vertically, relative to the light path, to permit various portions of the flame to be examined.

The burner was housed in a chamber with a single exhaust port through which the flame products were removed by means of a vacuum-pressure pump. The burner exhaust gases were drawn through an aerosol filter to a fume exhaust blower.

Emission spectra were observed for BeO in an oxyhydrogen flame in the region from 4000 cm^{-1} to 550 cm^{-1}. Since atmospheric and reaction water absorption masked the 4000-3400 cm^{-1} and the 1900-1300 cm^{-1} ranges, the only new emission bands observed were in the 600-700 cm^{-1} range. The band system is quite complex and is centered at 650 cm^{-1}. The band, as it appears (Fig. 23), could be a single frequency with complex rotational components, or several frequencies, and their rotational components. The spectrum (Fig. 23) was referenced against the spectrophotometer's internal glower. Both of these beams were reflected off the same mirrors and therefore had approximately the same path lengths. The sample beam, however, passes through an NaCl lens and an NaCl window of total thickness of ~10 mm.

Several experiments were performed employing this laboratory's three meter visible and U.V. grating spectrograph in an attempt to obtain the vibrational components of the electronic transitions of $Be(OH)_2$. A band had previously been reported resulting from flame emission spectra of beryllium salts in an oxyhydrogen flame located at 4710Å.[32] However, exposures of one hour (103af plates) employing the same flame apparatus that was used in the infrared measurements showed only a faint band in the 4650-4800Å region. The band appeared as a continuum with no apparent line structure.

C. Discussion

Employing the data obtained from the experimental spectroscopic investigation of $Be(OH)_2(g)$ in these laboratories, together with data from the literature, a calculation has been made for the entropy.

The calculation of the spectroscopic entropy requires a knowledge of the structure of gas molecules. When a complete rotational-vibrational spectra is available, the structure may be deduced from an analysis of the spectra.

Fig.

SPECTRUM $Be(OH)_2$

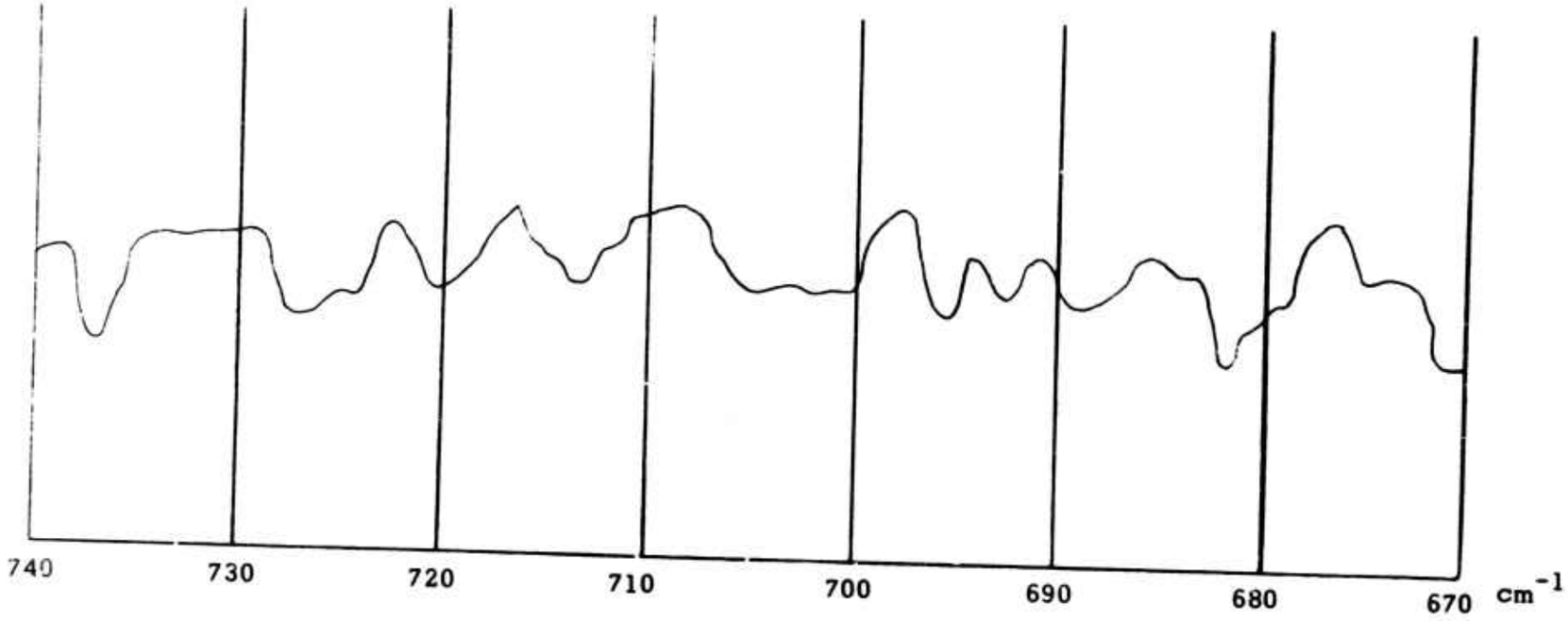

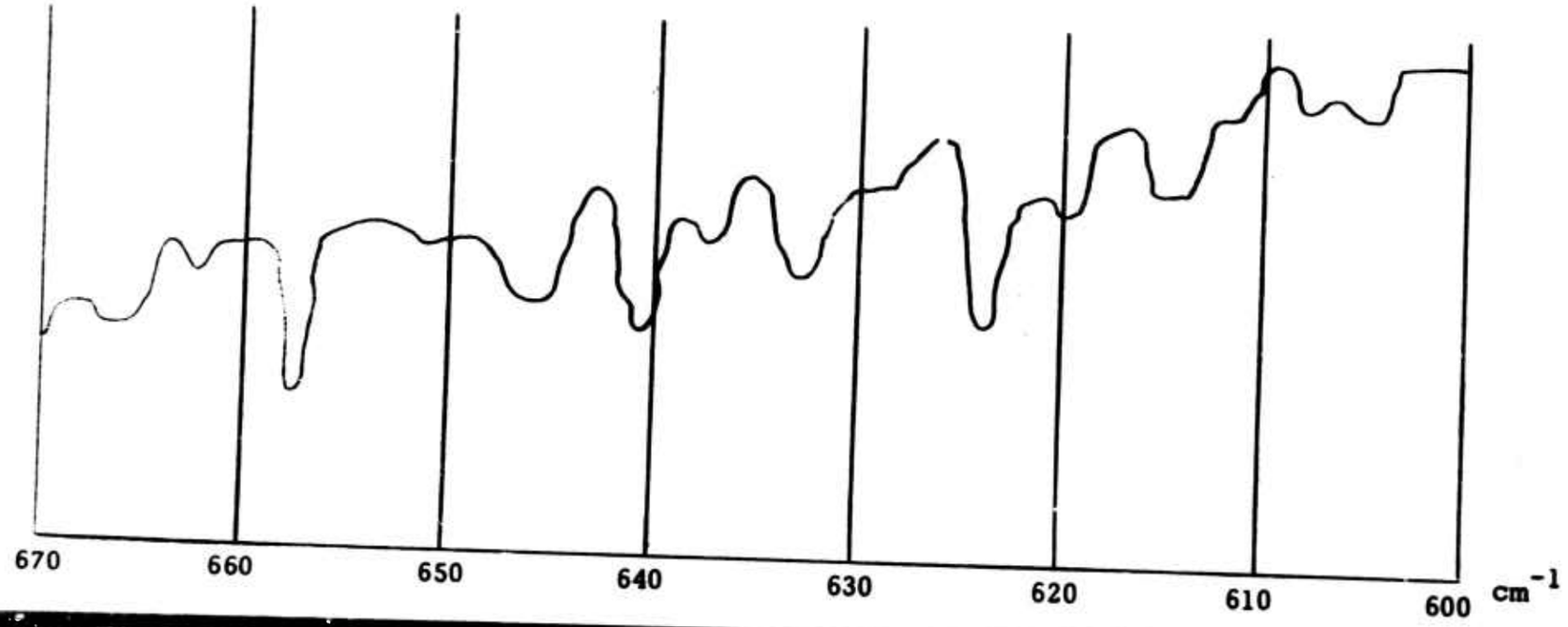

Since these spectra obtained were far from complete, a definite determination of the structure was not possible. Therefore, two molecular structural models have been assumed: a linear model, and a bent model. The bent model is the transconfiguration, but this form would give the same rotational contribution to the entropy as the cis, and the vibrational contributions would differ only slightly. The calculated entropies for the bent and linear forms may be sufficiently different, so that by comparison with the experimental values[5] the correct model may be distinguished. The calculation of the spectroscopic entropy for both models can be divided into three parts: translational, rotational, and vibrational. The electronic and nuclear spin contributions have been disregarded. The calculations are based on the harmonic-oscillator rigid rotator approximation. At 298°K this approximation is very satisfactory. At 1705°K the influence of anharmonicity will make itself felt and the calculated vibrational entropy will no longer give the accurate representation as it did at 298°K. However, this disregard of anharmonicity at 1705°K is negligible compared with the other approximations that have been made.

The translational entropy for both models is the same, since it depends only on the temperature and molecular weight of the gaseous $Be(OH)_2$. The value at 298.15°K is 37.190 cal/deg/mole, and at 1705°K it is 45.849 cal/deg/mole.

The rotational entropy calculation involves estimates of the bond angles and bond distances. For both models the Be-O distance has been taken to be 1.5A. The JANAF Tables use 1.4A in their calculations. Since BeF_2 has a bond distance of 1.43A and the double bond distance in BeO is 1.4A,[1] it seems unlikely that $Be(OH)_2$ would be the same as in these two molecules. The O-H distance has been taken to be 0.96A on the basis of compiled data.[33] Most oxygen bond angles are close to 105°: the smallest oxygen bond angle reported, 100°, is for OF_2.[33] Therefore, the Be-O-H angle has been taken to be 105°. This angle applies to the bent model. The linear model, of course, has an angle of 180°. The calculated rotational entropies for the bent model at 298°K and 1705°K are 20.597 and 25.792 cal/deg/mole, respectively. For the linear model these entropies are 14.397 and 17.860 cal/deg/mole. Fortunately, the moments of inertia, which depend on the bond angles and distances, represent roughly 15% of the rotational entropy in the bent case and 20% in the linear case. Errors of 0.1A and 5° in estimating the distances and angles in calculating the moments

of inertia result in about 1.4 cal/deg/mole or 5-6% error in the rotational entropies for the bent model. For the linear model the error in estimating leads to 0.5 cal/deg/mole or 2-3% error in the rotational entropies.

The vibrational entropy calculation requires a knowledge of the vibrational frequencies associated with the intramolecular motions of the molecule. On the basis of the two models (Fig. 24 and 25), the linear model should have seven frequencies independent of the cis or trans forms. A careful analysis of the frequencies of similar molecules was the basis for the assignment of values to these vibrational modes. The contribution to the vibrational entropy is greatest for the frequencies below 1000 cm^{-1}. As discussed in the experimental section, this investigation centered on this region to the lower limit of 550 cm^{-1}. Newkirk[34] has reported an O-H stretch of 3500 for $Be(OH)_2$. This data allows the assignment for frequencies of 3500 and 3600 which are the symmetric O-H stretching vibrations, ν_1, for both models and the asymmetric O-H stretch, ν_6, for the bent model and ν_3 for the linear model. This allows an assignment of 1600 as a reasonable frequency for the asymmetric BeO stretch of ν_7 (bent) and ν_4 (linear). Values of 1100 for an OH torsion ν_8 and 900 for Be-O symmetric stretch ν_2 have been selected for the bent model. A value of 900 for symmetric Be-O stretch ν_2 and 650 as an OH torsion ν_5 (doubly degenerate) for the linear model. The experimental value of 650 is either a unique frequency or a group of frequencies as discussed previously in the experimental section. Therefore, for the bent model, values of 700, 600 and 600 have been selected for Be-O bending, ν_3 Be-O bending ν_9 and OH torsion ν_4. For the linear model the value at 650 ν_6 (doubly degenerate) has been assigned as a Be-O bending mode. (These frequencies are listed in Table XIII).

$Be(OH)_2$ should have a slightly weaker force constant than BeF_2, however, the OH group has a mass of 17 compared to 19 for F. Therefore, the frequency of the low frequency mode in $Be(OH)_2$ should be quite close to that of BeF_2. Snelson[35] reports a frequency of 320 cm^{-1} for the BeF_2. Therefore, the value chosen for the low frequency mode, ν_7, for the linear model is 300 cm^{-1}. The remaining frequency, ν_5, for the bent model has been assigned a value of 300 cm^{-1} based on the bond character and distances between OH groups.

Based on these frequencies, the calculated vibrational entropy for the bent model yields values of 2.830 and 21.679 cal/deg/mole at 298°K and 1705°K, respectively. For the linear model the values are 4.463 at 298°K and

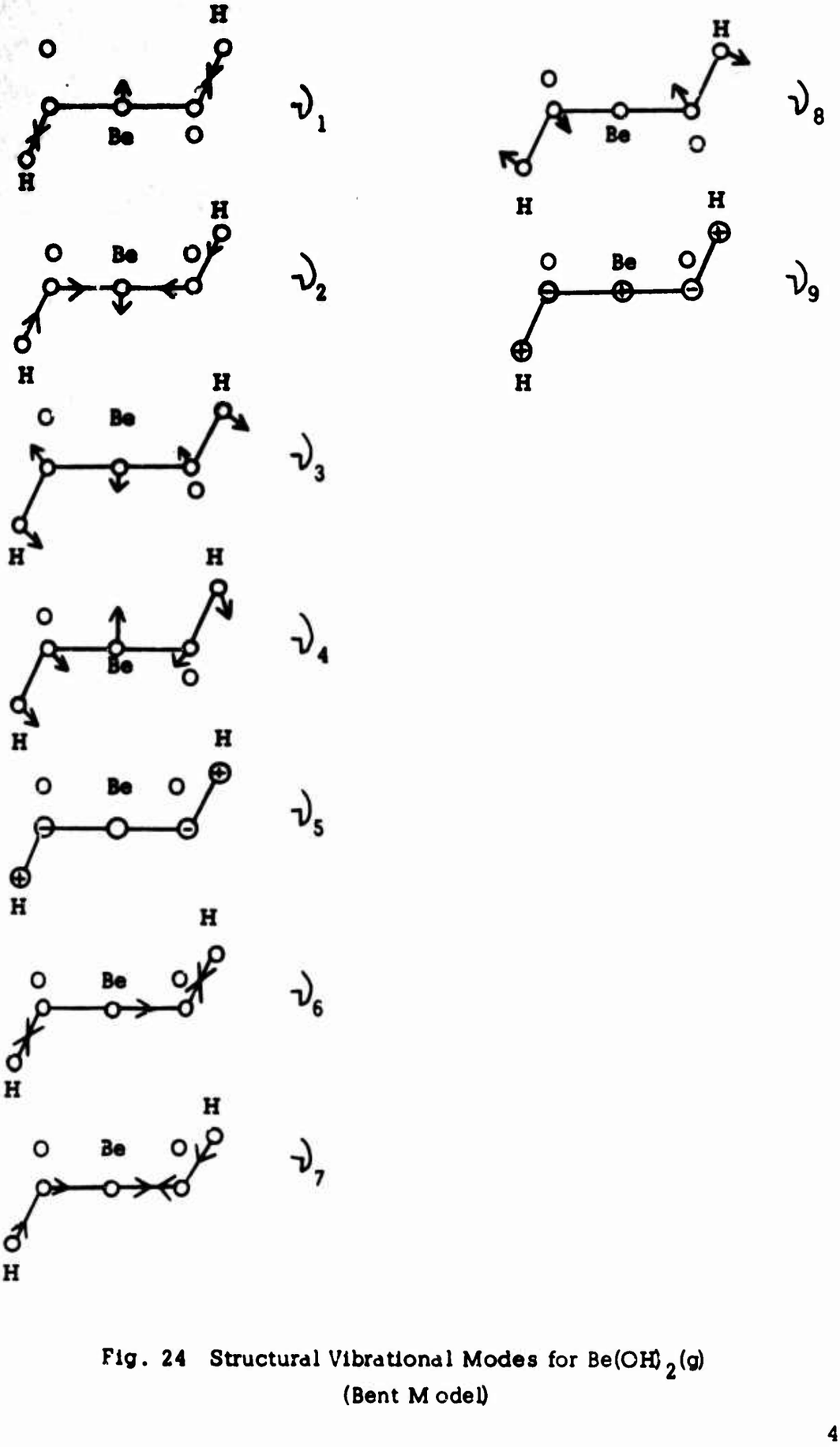

Fig. 24 Structural Vibrational Modes for $Be(OH)_2(g)$
(Bent Model)

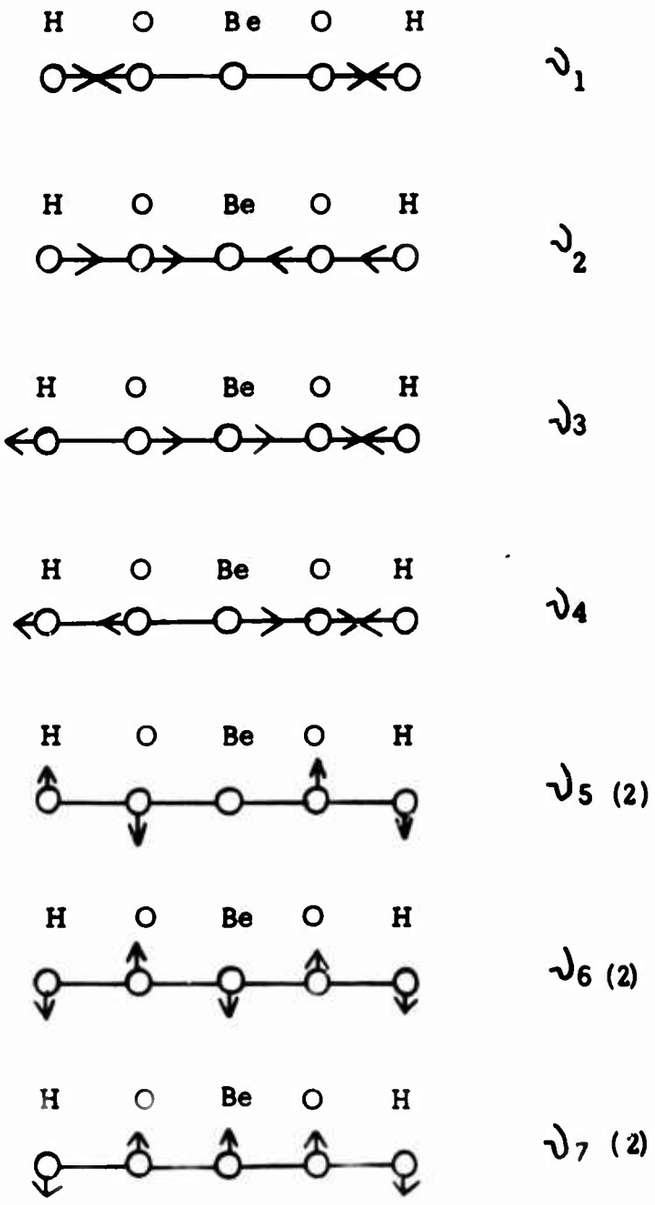

Fig. 25 Structural Vibrational Modes for $Be(OH)_2(g)$
(Linear Model)

27.231 cal/deg/mole at 1705°K. For a deviation of 100 cm^{-1} for each frequency in the bent model, the vibrational contribution to the entropy would change 0.8 e.u. at 298°K and 2.1 e.u. at 1705°K or approximately 30% at 298°K and 10% at 1705°K. For the linear model the changes would be 1.4 cal/deg/mole at 298°K and 2.1 cal/deg/mole at 1705°K or 30% and 8%. The choice of the 300 cm^{-1} rather than the 600 cm^{-1} choice of JANAF for one vibration contributes an additional 1.4 cal/deg/mole at 1705°K and 1.0 cal/deg/mole at 298°K for the bent model, and for the linear model they are 2.8 e.u. at 1705°K and 2.0 e.u. at 298°K.

The total discrepancies in entropy from the estimates of angles, distance and frequencies are 2.2 cal/deg/mole at 298°K and 3.5 cal/deg/mole at 1705°K for the bent model, which are roughly 4% of the total entropy. For the linear model the discrepancies are 1.9 cal/deg/mole at 298°K and 2.6 cal/deg/mole at 1705°K.

The resultant entropy at 298.15°K is 60.6 cal/deg/mole for the bent model and 56.1 cal/deg/mole for the linear model. At 1705°K the values are 93.3 cal/deg/mole for the bent model and 90.9 cal/deg/mole for the linear model.

The experimental value of Blauer, et al,[5] of 92.6 $\pm$ 4 cal/deg/mole at 1705°K is nearly equal to that of the bent model 93.3 e.u. and somewhat higher than that of the linear mode 90.9 e.u.

This new calculated entropy allows a re-examination of the third law heat of formation obtained by Blauer, et al.[5] If the calculated entropy for the bent model of 93.3 e.u. is used, then a third law value at 1705°K for $\Delta H_{f1705^\circ K}$ of $Be(OH)_2(g)$ of -166.4 kcal/mole is obtained. This is equal to the second law value at the average temperature of 1705°K. The third law value reduces to -160.9 $\pm$ .7 at 298°K.

REFERENCES

1. JANAF Thermochemical Tables.

2. D. L. Hildenbrand, et al, Final Technical Report, AFRPL-TR-65-95, Contract AF 04(611)-8523, April 1965.

3. JANAF Thermochemical Tables, December 31, 1960.

4. M. Farber, J. Chem. Phys. 36, 1101 (1962).

5. J. Blauer, M. A. Greenbaum and M. Farber, J. Phys. Chem. 70, 973 (1966).

6. E. Baur and R. Brunner, Helv. Chim. Acta. 17, 958 (1934).

7. C. L. McCabe and C. E. Birchenall, J. Metals, 5, 707 (1953).

8. R. B. Holden, R. Speiser and H. L. Johnston, J. Am. Chem. Soc. 70, 3897 (1948).

9. E. A. Gulbransen and K. F. Andrew, J. Electrochem. Soc. 97, 383 (1950).

10. A. N. Nesmeyanov, Vapor Pressure of the Chemical Elements, Ed. by R. Gary, Elsevier Publishing Co., 1963, p. 172.

11. S. Dushman, Vacuum Technique, John Wiley and Sons, Inc., New York, 1949.

12. Margaret A. Frisch, M. A. Greenbaum and M. Farber, J. Phys. Chem. 69, 3001 (1965).

13. P. Gross, C. S. Campbell, P. J. C. Kent and D. L. Levi, Disc. Fara. Soc., 4, 206 (1948).

14. A. S. Russell, K. E. Martin, and C. N. Cochran, J. Am. Chem. Soc. 73, 1466 (1951).

15. S. A. Semenkovich, Zh. Prikl, Khim., 33, 1281 (1960); Chem. Abstr. 54, 1925d (1960).

16. D. Bhogeswara Rao and V. V. Dadape, J. Phys. Chem. 70, 1349 (1966).

17. A. G. Gaydon, Dissociation Energies and Spectra of Diatomic Molecules, Chapman and Hall, Ltd., London, 1953.

18. W. P. Sholette and R. F. Porter, J. Phys. Chem. 67, 177 (1963).

19. A. Buchler and J. B. Berkowitz-Mattuck, J. Chem. Phys. 39, 286 (1963).

20. D. L. Hildenbrand, W. F. Hall and N. D. Potter, J. Chem. Phys. 39, 296 (1963).

21. M. D. Sheer, J. Phys. Chem. 61, 1184 (1957).

22. D. White, P. N. Walsh, H. W. Goldstein and D. F. Dever, J. Phys. Chem. 65, 1404 (1961).

23. A. Sommer, Ph.D. Thesis, The Ohio State University, 1962.

24. P. E. Blackburn, Arthur D. Little, Inc. Quarterly Report No. 4, Mar 1 - May 31, 1963, "Research on Thermodynamics of the Al-B-O and Be-B-O Systems."

25. John L. Margrave and Associates, "Molecular Parameters and Thermodynamic Properties of Light Element Molecules," Proceedings of the Third Meeting, ICRPG Working Group on Thermochemistry, March 1965.

26. O. J. Meschi, W. A. Chupka, and J. Berkowitz, J. Chem. Phys. 33, 530 (1960).

27. D. White, D. C. Mann, P. N. Walsh and A. Sommer, J. Chem. Phys. 33, 488 (1960).

28. M. Farber, et al, Final Technical Report, Contract DA-04-495-ORD-1987, May 1960 through June 1962, Rocket Power, Inc.

29. JANAF Thermochemical Tables, March 31, 1961.

30. L. I. Grossweiner and R. L. Seifert, J. Am. Chem. Soc. 74, 2701 (1952).

31. W. A. Young, J. Phys. Chem. 64, 1003 (1960).

32. Beckman Instruments, Inc. Bulletin No. 736c.

33. L. Pauling, The Nature of the Chemical Bond, Cornell University Press, Ithaca, N. Y. (1951), p. 168.

34. H. W. Newkirk, Inorg. Chem. 3, 1041 (1964).

35. A. Snelson, IITRI Report C6013-3, Contract DA-31-124-ARO(D).

TABLE I

EFFUSION CELL CHARACTERISTICS

	Diameter of Effusion Hole	Depth of Hole	Clausing Factor, W_o
Cell No. 1	1.065 mm	1.27 mm	0.471
Cell No. 2	0.990 mm	2.0 mm	0.359

TABLE II

EXPERIMENTAL DATA OF MOLECULAR FLOW EFFUSION EXPERIMENTS

Run No.	T (°K)	Time (min)	Total Wt. Loss of BeO (mg)	Blank (mg)	Total Moles of H_2 x 10^2	Net Wt. Loss of BeO (110 min)	No. of Moles of H_2 (110^2 min)
29**	2107	290	6.1	0.2	3.567	2.24	1.353
5**	2139	230	7.0	0.5	2.459	3.11	1.176
30**	2139	230	7.2	0.5	2.840	3.20	1.358
6**	2171	230	8.9	1.2	2.344	3.68	1.121
7**	2171	230	9.0	1.2	2.524	3.73	1.207
8**	2171	230	8.7	1.2	2.944	3.59	1.408
9**	2203	110	5.8	1.0	1.372	4.80	1.372
10**	2203	230	12.1	2.6	2.745	4.54	1.313
11**	2235	110	8.5	2.5	1.487	6.0	1.487
12**	2235	110	8.0	2.0	1.372	6.0	1.372
13**	2235	230	18.4	5.0	2.613	6.41	1.250
14**	2235	230	17.0	5.0	2.548	5.74	1.218
15**	2268	110	11.9	4.3	1.425	7.60	1.425
17*	2268	110	13.3	2.2	1.487	11.1	1.487
18*	2268	110	11.4	2.2	1.434	9.2	1.434
19*	2268	110	12.0	2.2	1.449	10.0	1.449
16**	2301	110	14.6	5.2	1.349	9.4	1.349
20*	2301	110	21.1	4.3	1.420	16.8	1.420
21*	2301	110	20.9	4.3	1.420	16.6	1.420
22*	2301	110	19.8	4.3	1.482	15.5	1.482
23*	2335	110	25.8	6.8	1.430	19.0	1.430
24*	2335	110	27.6	6.8	1.415	20.8	1.415
25*	2368	110	31.8	8.5	1.372	23.3	1.372
26*	2368	110	30.0	8.5	1.377	21.5	1.377

* Cell 1

** Cell 2

TABLE III

CALCULATED DATA FOR THE REACTION

$BeO(c) + 1/2H_2(g) = BeOH(g)$

Run No.	T (°K)	Loss of BeO (mg/110 min)	P_{Be}, atm x 10^6	Be Wt. Loss due to Be Formation (mg/110 min)	BeO Wt. Loss due to BeOH Formation (mg/110 min)	P_{H_2}, atm x 10^4	P_{BeOH}, atm x 10^5	$K_2 \times 10^3$
29**	2107	2.24	1.94	0.28	1.96	10.29	22.69	0.707
5**	2139	3.11	2.36	0.34	2.77	8.849	3.232	1.086
30**	2139	3.20	2.55	0.37	2.83	10.28	3.302	1.029
6**	2171	3.68	2.99	0.43	3.25	8.362	3.821	1.322
7**	2171	3.73	3.12	0.45	3.28	9.031	3.856	1.283
8**	2171	3.59	3.38	0.49	3.10	10.61	3.644	1.120
9**	2203	4.80	4.30	0.62	4.18	10.22	4.949	1.546
10**	2203	4.54	4.19	0.60	3.94	9.773	4.665	1.495
11**	2235	6.0	5.71	0.81	5.19	10.99	6.188	1.867
12**	2235	6.0	5.46	0.78	5.27	10.08	6.224	1.957
13**	2235	6.41	5.18	0.74	5.67	9.129	6.761	2.239
14**	2235	5.74	5.11	0.73	5.01	8.890	5.974	2.005
15**	2268	7.60	7.09	1.00	6.60	10.34	7.929	2.466
17*	2268	11.1	5.72	1.23	9.87	6.905	7.825	2.981
18*	2268	9.2	5.61	1.20	8.0	6.690	6.342	2.453
19*	2268	10.0	5.64	1.21	8.79	6.712	6.969	2.691
16**	2301	9.4	8.63	1.21	8.19	9.534	9.913	3.213
20*	2301	16.8	6.94	1.48	15.32	6.336	12.24	4.857
21*	2301	16.6	6.94	1.48	15.12	6.342	12.08	4.794
22*	2301	15.5	7.12	1.52	13.98	6.663	11.17	4.329
23*	2335	19.0	8.67	1.83	17.17	6.176	13.82	5.573
24*	2335	20.8	8.59	1.32	18.98	6.082	15.27	6.195
25*	2368	23.3	10.27	2.16	21.14	5.621	17.14	7.232
26*	2368	21.5	10.32	2.17	19.33	5.666	15.67	6.584

* Cell 1

** Cell 2

TABLE V

FREE ENERGY AND HEAT OF REACTION FOR THE EQUILIBRIUM

$$BeO(c) + 1/2H_2(g) = BeOH(g)$$

$T^{\circ}K$	ΔF_r (kcal)	ΔH_r (kcal)	ΔH_r^{298} (kcal)
2107	30.37	87.207	94.603
2139	29.01	86.553	94.109
2139	29.25	86.788	94.344
2171	28.59	86.834	94.549
2171	28.73	86.973	94.688
2171	29.32	87.560	95.275
2203	28.34	87.276	95.151
2203	28.48	87.418	95.293
2235	27.91	87.542	95.580
2235	27.70	87.328	95.366
2235	27.10	86.734	94.772
2235	27.59	87.225	95.262
2268	27.07	87.947	96.153
2268	26.22	86.556	94.762
2268	27.10	87.438	95.644
2268	26.67	87.012	95.218
2301	26.26	87.308	95.684
2301	24.37	85.413	93.789
2301	24.31	85.360	93.736
2301	24.88	85.929	94.305
2335	24.08	85.821	94.409
2335	23.59	85.329	93.917
2368	23.20	85.602	94.395
2368	23.64	86.046	94.839

TABLE V

SUMMARY OF THERMODYNAMIC DATA FOR THE REACTION

$BeO(c) = 1/2H_2(g) = BeOH(g)$

$\Delta H^{o}_{r2235^{o}K}$	88.3 ± 3.8 kcal	87.2 ± 0.5 kcal
$\Delta H^{o}_{r298^{o}K}$	96.3 ± 3.8 kcal	94.9 ± 0.5 kcal
$\Delta H^{o}_{f2235^{o}K}$ BeOH(g)	-55.7 ± 3.8 kcal/mole	-56.7 ± 0.5 kcal/mole
$\Delta H^{o}_{f298^{o}K}$ BeOH(g)	-46.8 ± 3.8 kcal/mole	-48.2 ± 0.5 kcal/mole
$\Delta S^{o}_{r2235^{o}K}$	27.4 ± 1.7 cal/deg/mole	
$S^{o}_{2235^{o}K}$ BeOH(g)	75.3 ± 1.7 cal/deg/mole	
$S^{o}_{298^{o}K}$ BeOH(g)	54.0 ± 1.7 cal/deg/mole	53.29 cal/deg/mole (JANAF)

TABLE VI

EXPERIMENTAL DATA FOR THE REACTION OF $AlCl_3$ VAPOR AND Al(s,l)

$T^{\circ}K$	Time (hrs)	Wt. Loss of $AlCl_3$ (gm)	Wt. Loss of Al (mg)	Flow of A (cc/hr)	Moles of A/hour $(N_A) \times 10^2$	Moles of Al/hour (wt. loss) $(N_{Al}) \times 10^5$
800	6.0	28.85	5.9	1338	5.48	3.643
800	6.0	47.95	8.7	1338	5.48	5.370
800	5.0	54.41	6.3	1440	5.91	4.670
800	5.0	34.10	4.0	1482	6.07	2.960
800	3.0	29.08	3.9	1030	4.22	4.820
800	0.67	11.00	1.7	1026	4.20	9.450
800	5.0	16.99	2.3	938	3.85	1.705
825	5.0	38.20	25.7	1338	5.48	4.220
825	5.0	28.05	4.6	1338	5.48	3.410
851	5.0	47.05	8.9	1060	4.34	6.590
851	4.5	36.33	6.0	1020	4.18	4.930
851	3.5	23.70	4.8	1092	4.47	5.070
875	5.0	29.05	6.2	912	3.74	4.600
875	3.0	25.80	5.6	1194	4.90	6.910
875	4.0	36.90	7.8	1194	4.90	7.225
901	4.5	26.10	7.7	913	3.74	6.330
901	4.0	26.55	7.5	956	3.92	6.960
901	4.0	24.22	7.3	1020	4.18	6.780
925	4.0	30.90	17.2	1338	5.48	15.94
925	4.0	37.40	11.0	1194	4.90	10.20
925	4.0	23.02	10.6	1194	4.90	9.82
949	3.0	18.35	15.5	1338	5.48	19.15
949	5.0	11.07	7.7	1290	5.29	5 71
949	1.25	13.41	5.1	942	3.86	15.10
949	2.5	21.47	10.2	942	3.86	15.10
975	3.0	26.80	19.7	1338	5.48	24.35
975	3.5	39.00	26.3	1338	5.48	27.85
975	4.0	22.33	15.5	1250	5.12	14.38
975	3.0	29.40	21.4	1338	5.48	26.42
1000	4.0	39.45	38.9	1338	5.48	36.00
1000	4.0	30.65	29.9	1338	5.48	27.65

TABLE VII

EQUILIBRIUM DATA FOR THE REACTION OF $AlCl_3$ AND Al

$T^{O}K$	K_4	N_{AlCl_3} x 10^2 (hr)	$N_{Al_2Cl_6}$ x 10^3 (hr)	K_1	$N_{Al} \times 10^5$ per hr due to Reaction (1)	K_5	$N_{Al} \times 10^5$ per hr due to Reaction (5)	$N_{Al} \times 10^5$ per hr due to Reaction (6)	K_6 x 10^8	Average Log K_6
800	0.199	1.335	11.40	4.34×10^{-14}	0.098	3.2×10^{-12}	0.119	3.433	34.20	
800	0.199	1.950	20.30	4.34×10^{-14}	0.131	3.2×10^{-12}	0.162	5.077	28.90	
800	0.199	2.490	28.45	4.34×10^{-14}	0.160	3.2×10^{-12}	0.205	4.306	07.83	
800	0.199	1.780	16.75	4.37×10^{-14}	0.128	3.2×10^{-12}	0.153	2.679	06.16	-6.84
800	0.199	2.120	25.30	4.37×10^{-14}	0.216	3.2×10^{-12}	0.168	4.436	12.98	
800	0.199	3.320	45.40	4.37×10^{-14}	0.184	3.2×10^{-12}	0.251	9.016	24.55	
800	0.199	0.937	08.09	4.37×10^{-14}	0.072	3.2×10^{-12}	0.084	1.550	09.12	
825	0.323	2.310	17.20	3.90×10^{-13}	0.289	1.446×10^{-11}	0.301	3.630	05.39	-7.23
825	0.323	1.814	12.03	3.90×10^{-13}	0.247	1.446×10^{-11}	0.246	2.917	06.57	
851	0.523	3.110	19.80	2.82×10^{-12}	0.613	6.31×10^{-11}	0.597	5.380	05.40	
851	0.523	2.740	16.60	2.82×10^{-12}	0.553	6.31×10^{-11}	0.532	3.845	02.92	-7.35
851	0.523	2.388	13.21	2.82×10^{-12}	0.511	6.31×10^{-11}	0.478	4.081	05.77	
875	0.845	3.690	16.25	1.70×10^{-11}	1.247	2.28×10^{-10}	1.055	4.923	02.22	
875	0.845	3.500	14.85	1.70×10^{-11}	1.197	2.28×10^{-10}	1.008	4.705	02.32	-7.66
875	0.845	2.418	09.76	1.70×10^{-11}	0.852	2.28×10^{-10}	0.706	3.042	01.98	

continued

TABLE VII - continued

$T^{\circ}K$	K_4	N_{AlCl_3} x 10^2 (hr)	$N_{Al_2Cl_6}$ x 10^3 (hr)	K_1	N_{Al} x 10^5 per hr due to Reaction (1)	K_5	N_{Al} x 10^5 per hr due to Reaction (5)	N_{Al} x 10^5 per hr due to Reaction (6)	K_6 x 10^8	Average Log K_6
901	1.370	2.925	08.13	9.34×10^{-11}	1.720	8.42×10^{-10}	1.293	3.767	01.95	
901	1.370	3.154	09.23	9.34×10^{-11}	1.774	8.42×10^{-10}	1.352	3.861	01.57	-7.76
901	1.370	2.800	07.80	9.34×10^{-11}	1.608	8.42×10^{-10}	1.214	3.508	01.74	
925	2.000	3.168	05.76	4.57×10^{-10}	3.170	2.57×10^{-9}	2.020	4.630	02.88	
925	2.000	2.726	04.87	4.57×10^{-10}	2.820	2.57×10^{-9}	1.766	3.934	02.90	-7.59
925	2.000	4.144	08.33	4.57×10^{-10}	7.830	2.57×10^{-9}	2.580	5.530	02.02	
949	2.920	1 450	01.08	1.78×10^{-9}	3.345	7.4×10^{-9}	1.580	0.785	00.25	
949	2.920	5.254	09.98	1.78×10^{-9}	6.175	7.4×10^{-9}	4.150	5.980	00.90	-8.40
949	2.920	4.806	08.32	1.78×10^{-9}	6.210	7.4×10^{-9}	3.920	5.170	00.83	
949	2.920	5.892	10.94	1.78×10^{-9}	6.850	7.4×10^{-9}	4.690	3.560	00.14	
975	4.270	5.990	06.90	6.31×10^{-9}	11.830	2.2×10^{-8}	7.090	7.970	01.61	
975	4.270	3.534	03.33	6.31×10^{-9}	8.120	2.2×10^{-8}	4.505	1.745	00.10	-8.23
975	4.270	6.743	08.16	6.31×10^{-9}	12.880	2.2×10^{-8}	7.850	7.120	00.77	
975	4.270	5.494	06.13	6.31×10^{-9}	11.730	2.2×10^{-8}	6.580	6.040	00.95	
1000	6.250	5.028	03.66	2.0×10^{-8}	15.330	5.92×10^{-8}	8.450	3.870	00.33	-8.21
1000	6.250	6.365	05.23	2.0×10^{-8}	17.940	5.92×10^{-8}	10.310	7.750	01.18	

TABLE VIII

THERMODYNAMIC DATA FOR $AlCl_2(g)$ AND $Al_2Cl_4(g)$

$\Delta H_{f900^\circ K} Al_2Cl_4(g)$	-194.8 ± 1.0 kcal/mole
$S^\circ_{900^\circ K} Al_2Cl_4(g)$	-115.7 ± 1.1 cal/deg/mole
$\Delta H_{f298^\circ K} Al_2Cl_4(g)$	-194 ± 5 kcal/mole
$S^\circ_{298^\circ K} Al_2Cl_4(g)$	90 ± 5 cal/deg/mole
$\Delta H_{f298^\circ K} AlCl_2(g)$	-66 ± 3 kcal/mole

TABLE IX

EQUILIBRIUM DATA FOR THE REACTION

$AlCl_3(g) + AlCl(g) = 2AlCl_2(g)$

T^oK	P_{AlCl_3} (atm)	P_{AlCl} (atm)	P_{AlCl_2} (atm)	% $AlCl_2$ Compared to AlCl
850	3.0×10^{-5}	4.2×10^{-6}	3.9×10^{-7}	8.4%
1000	3.7×10^{-5}	8.2×10^{-5}	4.3×10^{-6}	5.0%

TABLE X

(D_2 Pressure = 75 μ)

A TYPICAL MASS SPECTROMETRIC DETERMINATION OF

THE SPECIES RESULTING FROM THE REACTION $B_2O_3(l)$ AND $D_2(g)$

T	1/T	Mass 20	Mass 29	Mass 45	Mass 70					
^oK	x 10^3	I_{D_2O}	I_{DBO}	I_{DOBO}	$I_{B_2O_3}$	K_1	log K_1	K_2	log K_2	log K_3
1161.1	.8380	75.	165.	15.		2.48×10^3	3.393	3.00	0.477*	
1187.3	.8200	110.	275.	25.5		7.01×10^3	3.846	5.20	0.772*	
1213.8	.8026	150.	405.	48.		1.94×10^4	4.288	1.54×10^1	1.188*	
1240.4	.7859	195.	570.	88.5		5.04×10^4	4.702	4.02×10^1	1.604*	
1267.2	.7698	270.	810.	145.5		1.18×10^5	5.072	7.84×10^1	1.894*	
1294.3	.7542	375.	1170.	265.	9.0	3.10×10^5	5.491	1.87×10^2	2.272	0.954*
1321.5	.7392	525.	1635.	435.	19.5	7.11×10^5	5.85[illegible]	3.60×10^2	2.556	1.290
1349.4	.7246	750.	2250.	690.	38.	1.55×10^6	6.190	6.35×10^2	2.803	1.580
1377.3	.7106	1000.	3200.	1110.	72.	3.55×10^6	6.550	1.23×10^3	3.090	1.857
1405.5	.6970	1300.	3900.	1710.	135.	6.67×10^6	6.824*	2.25×10^3	3.352	2.130

*Discarded

TABLE XI

INTENSITIES OF MAJOR SPECIES OF REACTION $B_2O_3(l) + D_2(g)$

(TEMP. 1518°K, PRESSURE 240 μ)

D_2O	2700	.23
BO	1260	.11
DBO	11850	1.00
BO_2	585	.049
DOBO	7600	.64
$B(OD)_2$	162	.014
$(BO)_2$	75	.0063
B_2O_3	555	.047

The trimers $(BOD)_3$ and $(DOBO)_3$ were not observed.

TABLE XII

THERMODYNAMIC DATA FOR THE REACTIONS

OF $P_2O_3(l)$ AND $D_2(g)$

Run	$D_2(g)$ μ	T avg. ^oK	ΔH_1 kcal/mole	T avg. ^oK	ΔH_2 kcal/mole	T avg. ^oK	ΔH_3 kcal/mole
1	75	1269	106.6 ± 0.5	1350	80.6 ± 1.3	1364	85.1 ± 0.2
2	75	1256	103.7 ± 0.9	1329	82.9 ± 1.2	1364	86.2 ± 3.8
3*	240	1310	96.4 ± 0.9	1270	80.9 ± 0.8	1364	$84.8 \pm .3$
4*	240	1271	100.2 ± 0.7	1271	80.1 ± 1.2	1351	85.2 ± 1.0
5	18	1215	104.0 ± 1.1	1296	79.5 ± 1.2	1324	84.2 ± 0.6
6	18	1245	102.1 ± 0.6	1311	83.0 ± 0.8	1284	91.4 ± 6.8**
7	18	1296	103.5 ± 1.2			1298	85.1 ± 0.8
8	240	1311	98.8 ± 0.6			1338	88.9 ± 2.4
9	75	1257	106.4 ± 0.6			1298	88.3 ± 0.9
Average		1260	104.4 ± 1.5	1320	81.5 ± 1.5	1320	86.3 ± 1.5

*Run discarded

**Point discarded

TABLE XIII

ESTIMATED FREQUENCIES FOR $Be(OH)_2(g)$

Bent Model		Linear Model		
3600	ν_6	3600	ν_3	
3500	ν_1	3500	ν_1	
1600	ν_7	1600	ν_4	
1100	ν_8	900	ν_2	
900	ν_2	650	ν_6	(2)
700	ν_3	650	ν_5	(2)
600	ν_4	300	ν_7	(2)
600	ν_9			
300	ν_5			

Unclassified

Security Classification

DOCUMENT CONTROL DATA - R&D

(Security classification of title, body of abstract and indexing annotation must be entered when the overall report is classified)

1. ORIGINATING ACTIVITY (Corporate author) Rocket Power, Inc.	2a. REPORT SECURITY CLASSIFICATION Unclassified 2b. GROUP

3. REPORT TITLE

Investigation of the Thermodynamic Properties of Rocket Exhaust Products

4. DESCRIPTIVE NOTES (Type of report and inclusive dates)

Final Report, August 1, 1965 through July 31, 1966

5. AUTHOR(S) (Last name, first name, initial)

Farber, Milton; Ko, Hon Chung; Grenier, George
Greenbaum, Michael A.; Marantz, Laurence B.; Yates, Robert
Frisch, Margaret A.; Chai, Bong J.

6. REPORT DATE	7a. TOTAL NO. OF PAGES	7b. NO. OF REFS
September 1966	61 (Text)	35

8a. CONTRACT OR GRANT NO.	9a. ORIGINATOR'S REPORT NUMBER(S)
AF04(611)-10929 b. PROJECT NO. 3148 c. BPSN: 623148 d. Program Structure Nr.: 750G	9b. OTHER REPORT NO(S) (Any other numbers that may be assigned this report)

10. AVAILABILITY/LIMITATION NOTICES

This document is subject to special export controls and each transmittal to foreign governments or foreign nationals may be made only with prior approval of AFRPL (RPPR-STINFO), Edwards, Calif., 93523.

11. SUPPLEMENTARY NOTES	12. SPONSORING MILITARY ACTIVITY
	Department of the Air Force Air Force Rocket Propulsion Laboratory (AFSC) Edwards, California 93523

13. ABSTRACT

A thermodynamic research program for the period August 1, 1965 through July 31, 1966 resulted in thermal data for the high temperature stable species BeOH(g), HBO(g), B_2O_3(g), HOBO(g), $AlCl_2$(g) and Al_2Cl_4(g). In addition, infrared spectral data have been obtained for $Be(OH)_2$(g).

DD FORM 1 JAN 64 1473

Unclassified

Security Classification

Unclassified

Security Classification

14. KEY WORDS	LINK A		LINK B		LINK C	
	ROLE	WT	ROLE	WT	ROLE	WT
Thermodynamic properties; heats of formation; entropies; exhaust species; light metal compounds; beryllium compounds; aluminum compounds; boron compounds; chlorides; oxides.						

INSTRUCTIONS

1. ORIGINATING ACTIVITY: Enter the name and address of the contractor, subcontractor, grantee, Department of Defense activity or other organization *(corporate author)* issuing the report.

2a. REPORT SECURITY CLASSIFICATION: Enter the overall security classification of the report. Indicate whether "Restricted Data" is included. Marking is to be in accordance with appropriate security regulations.

2b. GROUP: Automatic downgrading is specified in DoD Directive 5200.10 and Armed Forces Industrial Manual. Enter the group number. Also, when applicable, show that optional markings have been used for Group 3 and Group 4 as authorized.

3. REPORT TITLE: Enter the complete report title in all capital letters. Titles in all cases should be unclassified. If a meaningful title cannot be selected without classification, show title classification in all capitals in parenthesis immediately following the title.

4. DESCRIPTIVE NOTES: If appropriate, enter the type of report, e.g., interim, progress, summary, annual, or final. Give the inclusive dates when a specific reporting period is covered.

5. AUTHOR(S): Enter the name(s) of author(s) as shown on or in the report. Enter last name, first name, middle initial. If military, show rank and branch of service. The name of the principal author is an absolute minimum requirement.

6. REPORT DATE: Enter the date of the report as day, month, year; or month, year. If more than one date appears on the report, use date of publication.

7a. TOTAL NUMBER OF PAGES: The total page count should follow normal pagination procedures, i.e., enter the number of pages containing information.

7b. NUMBER OF REFERENCES: Enter the total number of references cited in the report.

8a. CONTRACT OR GRANT NUMBER: If appropriate, enter the applicable number of the contract or grant under which the report was written.

8b, 8c, & 8d. PROJECT NUMBER: Enter the appropriate military department identification, such as project number, subproject number, system numbers, task number, etc.

9a. ORIGINATOR'S REPORT NUMBER(S): Enter the official report number by which the document will be identified and controlled by the originating activity. This number must be unique to this report.

9b. OTHER REPORT NUMBER(S): If the report has been assigned any other report numbers *(either by the originator or by the sponsor)*, also enter this number(s).

10. AVAILABILITY/LIMITATION NOTICES: Enter any limitations on further dissemination of the report, other than those imposed by security classification, using standard statements such as:

(1) "Qualified requesters may obtain copies of this report from DDC."

(2) "Foreign announcement and dissemination of this report by DDC is not authorized."

(3) "U. S. Government agencies may obtain copies of this report directly from DDC. Other qualified DDC users shall request through _____."

(4) "U. S. Military agencies may obtain copies of this report directly from DDC. Other qualified users shall request through _____."

(5) "All distribution of this report is controlled. Qualified DDC users shall request through _____."

If the report has been furnished to the Office of Technical Services, Department of Commerce, for sale to the public, indicate this fact and enter the price, if known.

11. SUPPLEMENTARY NOTES: Use for additional explanatory notes.

12. SPONSORING MILITARY ACTIVITY: Enter the name of the departmental project office or laboratory sponsoring *(paying for)* the research and development. Include address.

13. ABSTRACT: Enter an abstract giving a brief and factual summary of the document indicative of the report, even though it may also appear elsewhere in the body of the technical report. If additional space is required, a continuation sheet shall be attached.

It is highly desirable that the abstract of classified reports be unclassified. Each paragraph of the abstract shall end with an indication of the military security classification of the information in the paragraph, represented as *(TS), (S), (C), or (U)*

There is no limitation on the length of the abstract. However, the suggested length is from 150 to 225 words.

14. KEY WORDS: Key words are technically meaningful terms or short phrases that characterize a report and may be used as index entries for cataloging the report. Key words must be selected so that no security classification is required. Identifiers, such as equipment model designation, trade name, military project code name, geographic location, may be used as key words but will be followed by an indication of technical context. The assignment of links, rules, and weights is optional

GPO 886-551